Doctoral Thesis

Endoplasmic reticulum stress sensor Ire1 controls the heat shock response in methylotrophic yeast *Pichia pastoris*

（メタノール資化性酵母 *Pichia pastoris* では小胞体ストレスセンサーIre1 は熱ショック応答も制御する）

YASMIN NABILAH BINTI MOHD FAUZEE
Program of Biological Science
Graduate School of Science and Technology
Nara Institute of Science and Technology

Supervisor: Assoc. Prof. KIMATA Yukio
Laboratory of Microbial Interaction
Submission date (2023, July 26th)

Table of Contents

Table

Figure

ABSTRACT

Eukaryotic cells commonly carry the endoplasmic reticulum (ER), in which secretory proteins are folded and modified. Dysfunction or functional shortage of the ER, namely ER stress, provokes a cytoprotective transcription program called the unfolded protein response (UPR). The UPR is triggered by transmembrane ER-stress sensors including Ire1, which in many fungal species, acts as an endoribonuclease to splice and mature the mRNA encoding the transcription factor Hac1. The methylotrophic yeast *Pichia pastoris* (syn. *Komagataella phaffii*) is frequently employed for heterologous recombinant protein production, partly because it has a robust protein secretory system. Hence, it thus sounds an intriguing and important question how the ER function is controlled in *P. pastoris* cells. In this study, I therefore explored the UPR and its related factors in *P. pastoris*. Unlike the case of *Saccharomyces cerevisiae*, the *HAC1* mRNA was partially but considerably spliced even under non-stress conditions, probably due to the high protein secretion from *P. pastoris* cells. Moreover, here I note previously unknown role of Ire1. In *P. pastoris* cells, the *IRE1* knockout mutation (*ire1Δ*) and the *HAC1* knockout mutation (*hac1Δ*) caused only partially overlapping gene-expression change. Protein aggregation and the heat shock response (HSR) was induced in *ire1Δ* cells but not in *hac1Δ* cells. Moreover, Ire1 was further activated upon high-temperature culturing and seemed to confer heat-stress resistance to *P. pastoris* cell. Our findings shown here cumulatively demonstrate an intriguing case in which the UPR machinery controls cytosolic protein folding status and the HSR, which is known to be activated upon accumulation of unfolded proteins in the cytosol and/or the nuclei.

CHAPTER 1: INTRODUCTION

1.1 The endoplasmic reticulum (ER) and the unfolded protein response (UPR)

The endoplasmic reticulum (ER) is a membrane-bound subcellular compartment commonly found in eukaryotic cells. It acts as a location in and on which certain proteins and lipidic molecules are biosynthesized. Secretory proteins carrying the N-terminal ER-localization signal co-translationally enter the ER, where they are folded, modified and assembled before transported to cell surface via the Golgi apparatus [1, 2]. The disulphide-bond formation and N-glycosylation are prominent protein-modification reactions performed in the ER. To carry out these roles, the ER contains various resident proteins including the molecular chaperone BiP and protein disulphide isomerase (PDI).

Dysfunction or functional shortage of the ER is called ER stress and accompanied with accumulation of unfolded proteins in the ER [3, 4]. For instance, ER stress is induced when secretory proteins are excessively expressed. Moreover, chemicals or antibiotics that impair the disulphide-bond formation or N-glycosylation serve as potent ER-stress stimuli. Because ER-accumulated unfolded proteins aggregate in the ER, which is then further damaged, ER stress is toxic for cells [5]. Prolonged ER stress leads to cell death in mammalian cells and is linked to several neurodegenerative diseases such as Alzheimer's disease and Parkinson's disease[3]. ER stress is problematic also for industrial production of recombinant secretory proteins [6].

The ER bears sophisticated machineries that survey and control quality of proteins. For instance, unfolded (or misfolded) proteins are trapped by BiP and subjected to ER-associated protein degradation (ERAD) [7]. The ERAD machinery consists of multiple components for retrieval transport of ER client proteins [8] [9], which are then degraded by the proteasomes in the cytosol [8, 10].

Besides the ERAD, the unfolded protein response (UPR) is also known to contribute to mitigation of ER stress [5, 11, 12]. The UPR means to induce gene expression alongside ER stress and has been initially disclosed through frontier studies using yeast *Saccharomyces cerevisiae* as the model organism.

Ire1 is an ER-located type-I transmembrane protein and acts as an ER stress sensor that provokes the UPR in response to ER stress (Fig. 1). The luminal domain of Ire1, which faces on the ER lumen, is believed to be responsible for ER stress-dependent oligomerization and activation of Ire1. In non-stressed *S. cerevisiae* cells, BiP is bound to the luminal domain of Ire1 [13, 14]. While ER stress causes dissociation of BiP from Ire1, this contributes to but is not sufficient for oligomerization and activation of Ire1 [15]. Unfolded proteins accumulated in the ER are directly captured by the luminal domain of Ire1, which is then self-oligomerized [16-18]. Furthermore, the intrinsically disordered segment located at the N-terminus of Ire1 additionally functions to suppress activity of Ire1 under non-stress conditions [19]. Because of these multiple regulatory events, Ire1 provokes the UPR tightly dependent on ER stress in *S. cerevisiae* cells [20].

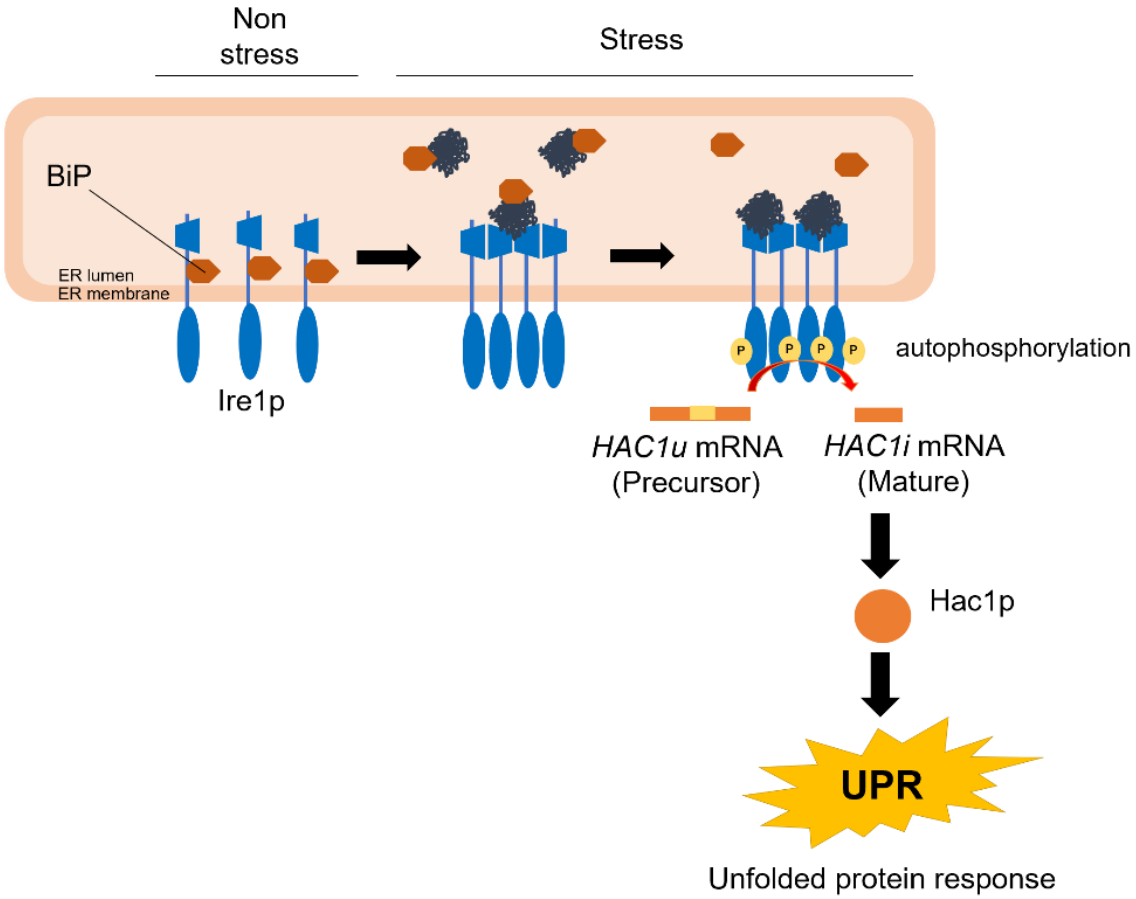

Figure 1: The UPR in *S. cerevisiae* cells

While the luminal domain acts as a regulatory module, the cytosolic domain has two enzymatic activities, namely the Ser/Thr kinase activity and endoribonuclease (RNase) activity, and acts as the effector module to trigger the UPR. When oligomerized dependently on the luminal domain under ER stress conditions, Ire1 is autophosphorylated [21], leading to its activation as an RNase [22, 23]. As shown in Fig. 1, Ire1 promotes splicing of the transcript of the *HAC1* gene, which hereafter I call the *HAC1*u mRNA ("u" stands for uninduced), in *S. cerevisiae* cells. The spliced form of the *HAC1* transcript, which hereafter I call the *HAC1*i mRNA ("i" stands for induced), is then translated to the transcription factor Hac1 [11].

Some of the prominent Hac1-target genes of *S. cerevisiae* cells including the BiP gene *KAR2* and the PDI gene *PDI1* carry the UPR element, to which Hac1 directly binds, on their promoter regions [24-26]. However, it is also likely that Hac1 induces more large numbers of genes, which mainly function for the ER [27]. The genes that transcriptionally induced by Hac1 upon ER stress include those encoding factors for protein translocation into the ER, for protein folding and modification (disulphide-bond formation and glycosylation) in the ER, for ERAD, and for vesicle transport that starts form the ER. In other words, functions of the ER and the protein secretory pathway are totally enhanced by the UPR.

Another UPR target gene in *S. cerevisiae* cells is *HAC1* itself [28]. When Ire1 is activated upon ER stress, Hac1 is highly produced, leading to the transcriptional induction of the *HAC1* gene. This posivive feedback is likely to conribute to mantenance of a high-level UPR upon long-term ER stress.

1.2 The UPR-inducing and other roles of Ire1

Ire1 is conserved throughout eukaryotic species. In ER-stressed animal cells, Ire1 carries out splicing of the XBP1 mRNA, the product of which is translated into a transcription factor that is involved in the UPR [29, 30]. A target of Ire1 in plant cells (*Arabidopsis*) is the ZIP60 mRNA [31, 32]. When not spliced by Ire1, the ZIP60 mRNA is translated into a membrane-anchored protein, which therefore cannot act as a transcription factor. On the other hand, the spliced form of the ZIP60 mRNA is translated into a soluble transcription factor that induces the UPR. Many, but not all, fugial species including yeasts carry the *HAC1* orthologues, the transcripts of which are spliced by Ire1 [33].

Kinase-dead mutants of Ire1 are able to induce the UPR if they take an appropriate structure for its activation as the RNase [34-37]. It is therefore likely that to provoke the UPR, the kinase motif of Ire1 functions only to activate the RNase motif of Ire1 [37, 38]. In other words, Ire1 does not phosphorylate other protein for the UPR induction.

Nevertheless, Ire1 seems to function not only as a RNase but also as a protein kinase to phosphorylate and activate c-Jun amino-terminal kinases (JNKs) in animal cells [39]. The ER stress-induced activatin of JNKs triggers apoptosis [40]. It is reasonable that sustained ER stress provokes apaotpsis in multicellular organisms, as irreversibly damaged cells are selectively and actively removed throhgh this process.

On the other hand, the most prominet role of Ire1 other than the UPR induction is the regulated Ire1-dependent decay (RIDD), for which its RNase motif functions. Hollien and Weissman [41] reported that in ER-stressed *Drosophila* cells, Ire1 mediates degradation of specific mRNAs, many of which encode ER client proteins. Therefore, protein load into the ER is likely to be decreased by the RIDD, resulting in mitigation of ER stress. It is today known that the RIDD occurs also in mammalian cells and plant cells [42-44]. Furthermore, Ire1 degrades certain microRNAs in ER-stressed mamalian cells, leading to apoptosis [45].

Unlike other fugal species well studied so far, *Schizosaccharomyces pombe* does not bear *HAC1*-gene orthologues. Kimmig et al. [46] demonstrated that the RIDD occurs in ER-stressed *S. pombe* cells without evocation of the conventional UPR. However, even in the case of *S. pombe* cells, BiP is induced upon ER stress. This is because in *S. pombe* cells, the BiP mRNA is stabilized through removal of its 3'-untranslated region by Ire1 [46].

In some other fungal species carrying *HAC1*-gene orthologues, Ire1 may also have a role(s) other than the splicing of the *HAC1* transcript. The UPR of pathogenic fungi and yeast is known to required for their virulence [47]. However, according to Feng et al. [48], the *IRE1* gene (IreA)-kockout mutant of filamentous fungus *Aspergillus fumigatus* exhibits more severe loss of the virulence than the *HAC1* gene (HacA)-kockout mutant. Moreover, the *IRE1*-kockout mutant of pathogenic yeast *Candida albicans* was more sensitive to iron depletion than the *HAC1*-knockout mutant [49]. Nevertheless, it is yet unclear how Ire1 works in these cases.

On the other hand, it is likely that in *S. cerevisaie* cells, the *HAC1*u mRNA is the sole target of Ire1 [50]. Tam et al. [51] reported *IRE1*-dependent but *HAC1*-independent decay of the *DAP2* mRNA, which however was not reproduced by my colleagues (data not shown). Furthermore, the *HAC1*u mRNA is virtually functionless unless it is converted to *HAC1*i mRNA by Ire1 [52]. In this context, the functions of *IRE1* and *HAC1* are highly

interdependent. Consequently, the *IRE1*-knockout and *HAC1*-knockout mutations exhibit identical phenotypes and do not exert additive or synergistic effects [53]. More recently, my colleagues suggested that in *S. cerevisiae* cells, Ire1 may have a target(s) other than the *HAC1*u mRNA, which, however, seems to be only minor (unpublished observation by Ho).

1.3 *Pichia pastoris*

Because of the re-classification based on its genome sequence, *Pichia pastoris* is now officially called *Komagataella phaffi* [54]. It is a methylotrophic yeast that can grow using methanol as a sole carbon and energy source. Although as well as *S. cerevisiae*, it belongs to the *Saccharomycetaceae* family in the Fungi kingdom, it is Crabtree-negative and requires molecular oxygen for healthy growth.

To utilize methanol, *P. pastoris* abundantly produces enzymes for methanol metabolism. For instance, the promoter of the *AOX1* gene, which encodes the alcohol oxidase, is robustly induced by methanol but repressed when other carbon sources are supplied. Because the *AOX1* promoter is extremely strong, it is frequently used as an inducible promoter for heterologous production of recombinant proteins [55].

Moreover, the Golgi apparatus in *P. pastoris* cells is stacked like that of mammalian cells, and is located adjacently to the ER [56]. This is a notable difference of *P. pastoris* cells from *S. cerevisiae* cells, in which the Golgi apparatus is dispersed through the cytoplasm. This observation may explain a reason why *P. pastoris* cells are suitable for protein secretion. In addition, the N-glycosylation chains in *P. pastoris* cells are less hyper-mannosylated than those in *S. cerevisiae cells* [57].

Having these advantageous properties, *P. pastoris* is today widely used for industrial production of recombinant secretory proteins [58]. The products include human secretory proteins, such as insulin, albumin, interferon, collagen, and antibody fragments, which are used as biopharmaceuticals (https://pichia.com/science-center/commercialized-products/). Many strategies are today taken to improve quality and quantity of proteins secreted form *P. pastoris* cells [58]. For instance, *P. pastoris* cells that can attach human-type N-linked sugar chains to secretory proteins have already been developed [59].

As described above, the secretory pathway, which starts from the ER, is controlled by the UPR. According to the total genome sequence data [60, 61], *P. pastoris* carries the *HAC1* gene and the *IRE1* gene respectively on

Chromosome 1 and Chromosome 3. As illustrated in Fig. 2, the *P. pastoris HAC1* gene has a 321 base intron sequence that is deduced to be removed by the Ire1-dependent splicing [62]. Fig. 3 shows amino-acid comparison of *P. pastoris* Ire1 against *S. cerevisiae* Ire1.

Intriguingly, artificial induction of the UPR machinery enhances the ER functions and is beneficial for industrial usage of *P. pastoris* cells. Unregulated and constitutive expression of the *HAC1*i mRNA occasionally results in modest enhancement of protein secretion [63].

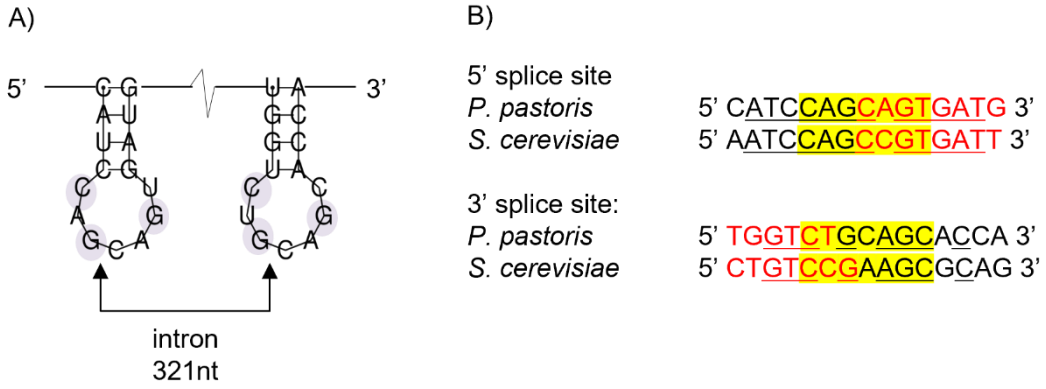

Figure 2: The splicing sites of the *P. pastoris HAC1* mRNA. (A) The stem-loop structure of the splicing sites of *P. pastoris HAC1* mRNA, which are attacked by Ire1. (B) The nucleotide sequence of the *HAC1* mRNA splicing sites is conserved between *P. pastoris* and *S. cerevisiae*. Red letters: the intron sequence.


Subregion 1
Subregion 2
Subregion 3
Subregion 4 -
Subregion 5
Transmembrane region
Pichia
Saccharomyces

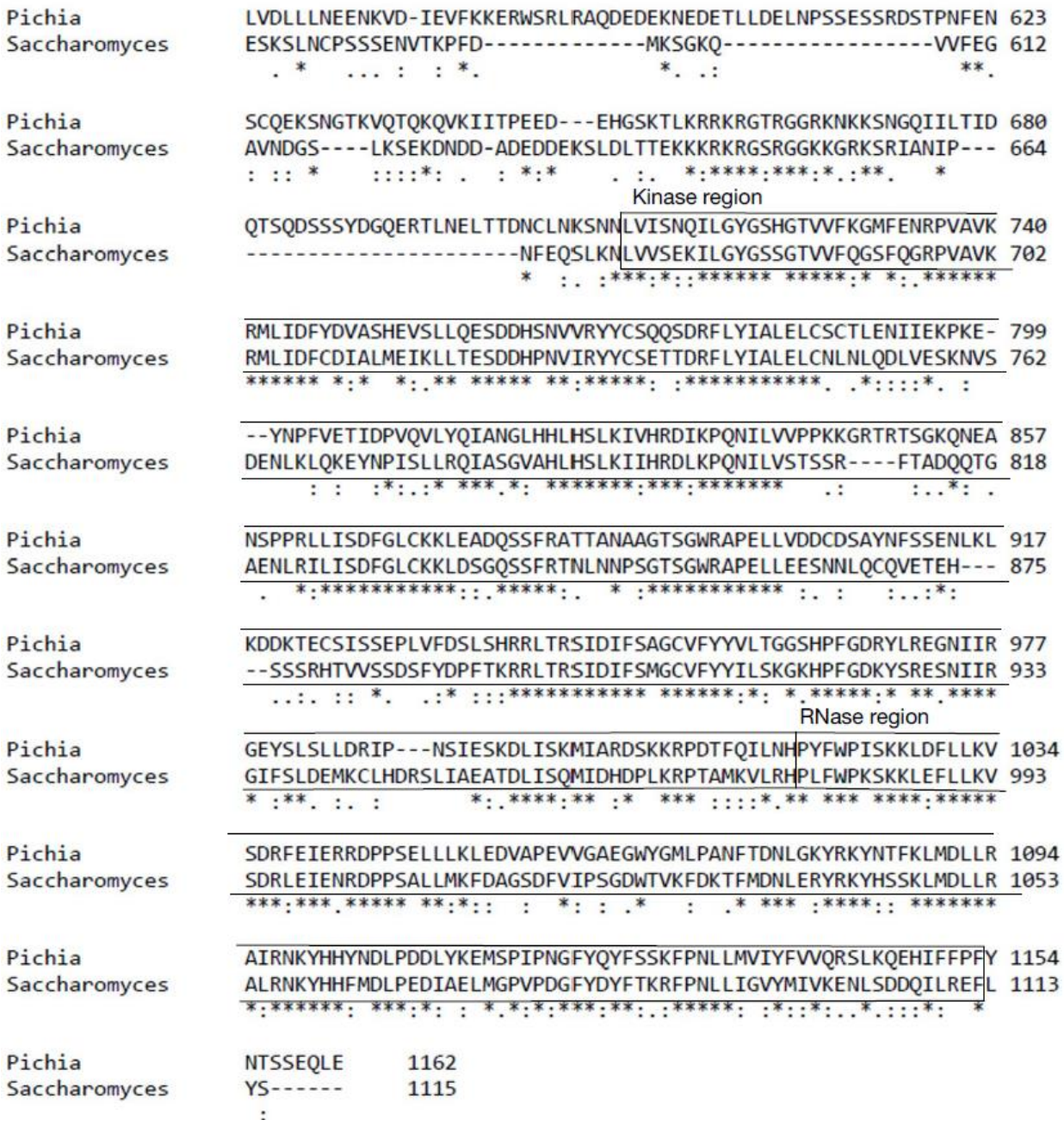

Figure 3: Comparison of the Ire1 amino acid sequence between *P. pastoris* and *S. cerevisiae*. The alignment was performed using Clustal Omega program in the Uniprot database. (*) indicates a fully conserved residue position. (:) indicates conservation between groups of strongly similar properties (scoring > 0.5 in the Gonnet PAM 250 matrix). (.) indicates conservation between groups of weakly similar properties (scoring =< 0.5 in the Gonnet PAM 250 matrix). (-) indicates the absence of corresponding amino acid residues at the positions. The black rectangles represent

the predicted functional domains of Ire1. The identity of full-length Ire1 amino-acid sequences between two species is 35.78%.

1.4 Purpose and outline of this study

In contrast to the remarkable advances of *P. pastoris* biotechnologies, physiological studies on *P. pastoris* do not seem to be well progressed. As for the UPR and its related molecules in *P. pastoris*, many questions remain unanswered. Guerfal et al. [62] proposed that in *P. pastoris* cells, the *HAC1*u mRNA is almost perfectly converted to the *HAC1*i mRNA even under non-stress conditions. This observation may suggest high and unregulated activation of *P. pastoris* Ire1. However, according to Whyteside et al. [64], the *HAC1* transcript remains unspliced under non-stress conditions, and is highly spliced strictly dependent on ER stress stimuli. Therefore, the ER-stress and Ire1-ativation status in *P. pastoris* cells is yet obscure. It is also uncovered if *P. pastoris* Ire1 has a role(s) other than the *HAC1*-mRNA splicing.

In my study, I therefore explored functions and regulations of the UPR-related molecules in *P. pastoris*, because my observations obtained here can be beneficial for industrial protein production from *P. pastoris* in the future. I then found that unlike the case of *S. cerevisiae* cells, splicing of the *HAC1* transcript by Ire1 partially but considerably occurs even under non-stress conditions, and are further stimulated by ER stress in *P. pastoris* cells. Moreover, in addition to the *HAC1*-mRNA splicing, Ire1 has another function to prevent protein aggregation in cytosol.

CHAPTER 2: MATERIALS AND METHODS

2.1 Genetic manipulation of *P.pastoris* cells

I used *P. pastoris* CBS7435 as the wild-type (WT) strain [60]. For transformation of *P. pastoris* cells, they were subjected to electroporation in accordance with Wu and Letchworth [65]. Genomic DNA samples were extracted using the Dr. GenTLE kit (Takara Bio, Kusatsu, Japan).

For the CRISPR/Cas9-based genome editing, I used plasmid BB3cK_pGAP_23*_pPFK300_Cas9, which carries the Cas9 nuclease gene, the guide RNA-expression module, and the G418-resistant kanMX marker [66]. DNA fragments carrying the guide RNA sequences (Table 1) were synthesized by Twist Bioscience (South San Francisco, CA, USA), and were ligated with BbsI-digeted BB3cK_pGAP_23*_pPFK300_Cas9 using the Gibson assembly kit (New England Biolabs, Ipswich, MA, USA). For generation of a donor DNA construct for the full-length *IRE1*-gene deletion (the *ire1Δ0* mutation), 5'- and 3'-flanking regions of the *IRE1* gene were PCR-amplified from genomic DNA respectively using primer sets I1/I4 and I3/I2 (Table 2), were fused by the Gibson assembly kit, and were PCR-amplified again using primer set I5/I6 (Table 2). For generation of a donor DNA construct for the full-length *HAC1*-gene deletion (the *hac1Δ0* mutation), 5'- and 3'-flanking regions of the *HAC1* gene were PCR-amplified from genomic DNA respectively using primer sets H1/H6 and H5/H2 (Table 2), were fused by the Gibson assembly kit, and were PCR-amplified again using primer set H7/H8 (Table 2). Subsequently, 1 μg of the resulting guide RNA/Cas9 expression plasmid and 5 μg of the resulting donor DNA construct were mixed and used for transformation of *P. pastoris* cells. The G418-resistant transformant clones were subjected to genomic PCR analysis using primer set I1/I2 or H1/H2 for confirmation of the *ire1Δ0* or *hac1Δ0* mutation, and were grown YPD not containing G418 for elimination of the guide RNA/Cas9 expression plasmid.

On the other hand, we also knocked out the *HAC1* gene and the *IRE1* gene through genomic insertion of the *kanMX* marker. By using primer sets H9/H10 and H11/H12 (Table 3), partial fragments of the *HAC1* gene were PCR-amplified from genomic DNA. The *kanMX* marker was PCR-amplified from BB3cK_pGAP_23*_pPFK300_Cas9 using primer set H13/H14 (Table 3). These three PCR products were fused by the Gibson assembly kit, and were PCR-amplified again using primer set H3/H4 (Table 3). Subsequently, the resulting *hac1::kanMX* gene-disruption module (*HAC1*-fragment (first half)-*kanMX*-*HAC1* fragment (latter half)) was used for transformation of *P. pastoris* cells, and the G418-resistant transformant clones were subjected to

genomic PCR analysis using primer set H3/H4 for confirmation of the *hac1::kanMX* mutation. The zeocin-resistant marker on the *IRE1*-knockout module described in Ref. [67] was replaced to the *kanMX* marker for generation of the *ire1::kanMX* allele.

Name	Sequence	Description
gRNA-IRE1 DNA	tcaattgaacaactatcaaaacaccatgGCAGATCTGATG AGTCCGTGAGGACGAAACGAGTAAGCTCGTC ATCTGCGTTTACTCATAATGGTTTTAGAGCTA GAAATAGCAAGTTAAAATAAGGCTAGTCCGT TATCAACTTGAAAAAGTGGCACCGAGTCGGT GCTTTTGGCCGGCATGGTCCCAGCCTCCTCG CTGGCGCCGGCTGGGCAACATGCTTCGGCAT GGCGAATGGGACAGCTTTGGACTgcttttagtgtac atctgataatatagt	Synthetic DNA fragment carrying the guide RNA targeting *IRE1*
gRNA-HAC1 DNA	tcaattgaacaactatcaaaacaccatgGTAATGCTGATG AGTCCGTGAGGACGAAACGAGTAAGCTCGTC CATTACAGCAGGCTCCATCGGTTTTAGAGCT AGAAATAGCAAGTTAAAATAAGGCTAGTCCG TTATCAACTTGAAAAAGTGGCACCGAGTCGG TGCTTTTGGCCGGCATGGTCCCAGCCTCCTC GCTGGCGCCGGCTGGGCAACATGCTTCGGCA TGGCGAATGGGACAGCTTTGGACTgcttttagtgt acatctgataatatagt	Synthetic DNA fragment carrying the guide RNA targeting *HAC1*

Table 1: Synthetic DNA fragments used to generate the guide RNA/Cas9 expression plasmids. The target gene-specific sequences are underlined. Sequences for hybridization to BbsI-digested BB3cK_pGAP_23*_pPFK300_Cas9 for the Gibson assembly ligation are indicated by lowercase letters.

Name	Direction	Sequence	Target	Final product
I1	Forward	**GCTTAATGGAAATCATTTGGTTCT**	5'-flanking region of *IRE1*	Donor DNA for the *ire1Δ0* allele
I4	Reverse	**tgaatggctacGATATAATTATCACTCACTGCAGG** (small letters: Sequence for annealing to the I3/I2 PCR product)	5'-flanking region of *IRE1*	
I3	Forward	**ataattatatcGTAGCCATTCAACTATGCACATAC** (small letters: Sequence for annealing to the I1/I4 PCR product)	3'-flanking region of *IRE1*	
I2	Reverse	**CTCCTTGATACTTCTATTATACTT**	3'-flanking region of *IRE1*	
I5	Forward	**CCTAGCCCTTTGAGTGCGTCTAGA**	5'-flanking region of *IRE1*	
I6	Reverse	**GAATATTCTTTTTCCTTTCTTCTC**	3'-flanking region of *IRE1*	
H1	Forward	**GATGGGAGCACATCAAGTGTAC**	5'-flanking region of *HAC1*	Donor DNA for the *hac1Δ0* allele
H6	Reverse	**ttaaatcaaaTTTTCTGCGATCTGATTCGACTAAG** (small letters: Sequence for annealing to the H5/H2 PCR product)	5'-flanking region of *HAC1*	
H5	Forward	**gatcgcagaaaATTTGATTTAAATGACTTTGTATT** (small letters: Sequence for annealing to the H1/H6 PCR product)	3'-flanking region of *HAC1*	
H2	Reverse	**CCCAAATTTCAATGCTTCCC**	3'-flanking region of *HAC1*	
H7	Forward	**CGCGCTATTCACCGCGAATAC**	5'-flanking region of *HAC1*	

H8	Reverse	**CTAACCTGTAAAGAGCTTGGC**	3'-flanking region of *HAC1*

Table 2: Oligonucleotide primers used for PCR to generate donor DNAs for the CRISR/Cas9-based genome editing.

Name	Direction	Sequence	Target	Product
H9	Forward	**AGACAGCTAGCCCACTTCCACCTCG**	*HAC1*	*HAC1* fragment (first half)
H10	Reverse	**gggcctccatgtcCTCCTGCTTGATAGATGTGCTC** (small letters: Sequence for annealing to the H13/H14 PCR product)	*HAC1*	
H13	Forward	**atcaagcaggagGACATGGAGGCCCAGAATACCC** (small letters: Sequence for annealing to the H9/H10 PCR product)	*kanMX*	*kanMX*
H14	Reverse	**atggagctgtagAGTATAGCGACCAGCATTCAC** (small letters: Sequence for annealing to the H11/H12 PCR product)	*kanMX*	
H11	Forward	**gtcgctatactCTACAGCTCCATCAGGTTCCATCA** (small letters: Sequence for annealing to the H13/H14 PCR product)	*HAC1*	*HAC1* fragment (latter half)
H12	Reverse	**GCATTAGCGGTAAATGGTGCTGC**	*HAC1*	
H3	Forward	**GAGCAAAGACGGAAGAAGAAAAGG**	*HAC1*	*hac1Δ::kanMX* module
H4	Reverse	**TTAACTACGCGTCTCGAACAAGGG**	*HAC1*	

Table 3: Oligonucleotide primers used for PCR to generate the *hac1Δ::kanMX* gene-deletion module.

2.2 Green fluorescent protein (GFP) expression in *P. pastoris* cells

As described below, plasmid pGHYB-GFP was created from the GFP expression plasmid pAHYB-GFP [68] through replacing its *AOX1* promoter to the *GAP1* promoter. The *GAP1* promoter was PCR-amplified from *P. pastoris* genome using oligonucleotide primer sets G1/G2 in Table 4 (capital letters: Sequence for annealing to the *GAP1* promoter region, underline letters: Artificially attached restriction sites (BglII and KpnI). Then, the PCR product and pAHYB-GFP were digested with BglII and KpnI and ligated.

The later obtained vector was confirmed by primer sets G3/G4 in Table 4. After linearization by cutting with BamHI, pGHYB-GFP was used for transformation of *P. pastoris* strains.

Purpose	Primer name		Primer sequence	PCR enzyme
Amplification of *P. pastoris* GAP1 promoter	G1	Forward	ccaagcagatctCTCTGCTACTCTGGTCCCAAGTG	Pyrobest
	G2	Reverse	ggctacggtaccTGTGTTTTGATAGTTGTTCAATT	
Verification of the GAP1-GFP vector	G3	Forward	TGGTTTCTCCTGACCCAAAG	Takara
	G4	Reverse	CCCCAGGATGTTGCCGTCCTCC	
The small letters represent the dummy short oligonucleotides followed by underlined letters represent the restriction site for its ligation to template vector				

Table 4: PCR primers used for GAP1-GFP vector construct

2.3 Growth and stress exposure of *P. pastoris* cells

For culturing *P. pastoris* cells, we used glucose-based rich medium (YPD medium) containing 1% yeast extract, 2% Bacto peptone and 2% glucose. Dithiothreitol (DTT) and tunicamycin were respectively purchased from Tokyo Chemical Industry (Tokyo, Japan) and from Sigma-Aldrich (Merck KGaA, Darmstadt, Germany). For agar plates, YPD was solidified by 2% agar. We used the spectrophotometer SmartSpec 3000 (BioRad, Hercules, CA, USA) to monitor optical density (OD_{600}) of cultures.

Unless otherwise noted, YPD cultures of *P. pastoris* cells were aerobically shaken at 30 °C, and cells in the exponentially growing phase were collected. To obtain DTT-treated cells, we added DTT solution (1M in water) into YPD cultures, which were further shaken at 30 °C for 30 min. For spot growth assay, YPD cultures (OD_{600}=1.0) were 10-fold serially diluted, and 1μL of cell suspensions were spotted onto agar plates.

2.4 *S. cerevisiae* strain, plasmids, genetic manipulation, and culturing

S. cerevisiae ire1Δ strain KMY1516 (*MATΔ ura3-52 LEU2::UPRE-CYC1 core promoter-GFP::leu2-3112 his3-Δ200 trp1-Δ901 LYS2::(UPRE)$_5$-CYC1 core promoter-lacZ::lys2-801 ire1Δ::TRP1*) has been described previously [69].

A single-copy YCp plasmid pRS313-IRE1 carries the *S. cerevisiae IRE1* gene (plus the 5′- and 3′-untranslated regions) into which the Sal I and Xba I restriction sites have been artificially introduced [15]. Two *S. cerevisiae IRE1*-gene fragments were PCR-amplified from pRS313-IRE1 using the primer sets S11/S12 and S15/S16 (Table 5). A *P. pastoris IRE1*-gene fragment was PCR-amplified from a *P. pastoris* genomic DNA plasmid using the primer set S13/S14 (Table 5). The resulting three PCR products were jointed using the overlap PCR technique (primer set S17/S18; Table 5). The products were mixed with Sal I/Xba I-digested pRS313-IRE1 and used for transformation of KMY1516 cells, which yielded a circular plasmid carrying the *P. pastoris*/*S. cerevisiae* chimeric *IRE1* gene via the *in vivo* homologous recombination [15]. For PCR, I used TaKaRa Pyrobest DNA polymerase.

The transformant cells were aerobically shaken at 30 °C in synthetic dextrose (SD) medium containing 2% glucose, Difco yeast nitrogen base w/o amino acids, and auxotrophic requirements.

Name	Direction	Sequence
S11	Forward	GAGATTAATCACATAGTAACAAGAA
S12	Reverse	GATGCCAAATCAACCATCGCATTTTTCAAAGTGCTAAAATATTAA
S13	Forward	TTAATATTTTAGCACTTTGAAAAATGCGATGGTTGATTTGGCATC
S14	Reverse	CTAGACTTCCAAACTTCAGTAGCAAAGGATAATTCTTGATACTGAGTTC
S15	Forward	GAACTCAGTATCAAGAATTATCCTTTGCTACTGAAGTTTGGAAGTCTAG
S16	Reverse	TCAGGTTTTCATCTGATACATTCTT
S17	Forward	CCATTATCACTTTTCTCCATATCA
S18	Reverse	CCTTGAAAACTTCCCTGAAAAACT

Table 5: Oligonucleotide primers used for PCR to generate the *P. pastoris/S. cerevisiae* chimeric *IRE1* gene. The *S. cerevisiae IRE1* gene-hybridization sequence is underlined. The *P. pastoris IRE1* gene-hybridization sequence is not underlined.

2.5 RNA analyses

Total RNA samples were extracted from *P. pastoris* cells and *S. cerevisiae* cells using the hot phenol method as described previously [37]. For conventional reverse transcription (RT)-PCR analysis to detect the *HAC1* mRNA, total RNA samples were subjected to RT reaction with the *HAC1*-specific RT primer P1 (or P2 for *S. cerevisiae*), which was followed by PCR with the *HAC1*-specific PCR primer set P3 and P4 (or S1 and S2 for *S. cerevisiae*) in accordance with our previous publication (Table 5) [67]. Because this PCR traversed the *HAC1* intron sequence, the spliced and unspliced forms of the *HAC1* mRNA yielded different-sized PCR products, which were then separated by agarose-gel electrophoresis in tris-borate-EDTA running buffer. Subsequently, ethidium bromide-fluorescent image of the gels was pictured with the digital imager E-box (Vilber Lourmat, Marne-la-Vallée, France).

Before the RT-quantitative PCR (RT-qPCR) and high-throughput RNA-seq analyses, residual DNA in total RNA samples was digested with recombinant DNase I (RNase-free; Takara, Kusatsu, Japan) in accordance with the manufacturer's instruction. Subsequently, DNase I was removed

from total RNA samples through phenol-chloroform extraction and ethanol precipitation.

For RT-qPCR analysis, total RNA samples were subjected to RT reaction using poly(dT) oligonucleotide primer (Table 6) and PrimeScript II Reverse Transcriptase (Takara, Kusatsu, Japan) as per manufacturer's instruction. The RT-reaction products were then analyzed by real-time qPCR as described previously [70] with the primer sets listed in Table 6. The *P. pastoris ACT1*-gene transcript was used as the reference [67], and the Ct method was used for calculation of relative gene expression levels.

Name	Purpose	Direction	Target	Sequence
P1	RT		*HAC1* (2^{nd} exon)	CATTAGCGGTAAATGGTGCTG
P2	RT		Universal	TTTTTTTTTTTTTTTTT
P3	PCR	Forward	*HAC1* (1st exon)	AGACAGCTAGCCCACTTCCACCTCG
P4	PCR	Reverse	*HAC1* (2nd exon)	CATTAGCGGTAAATGGTGCTG
S1	PCR	Forward	*S. cerevisiae HAC1* (1st exon)	TACAGGGATTTCCAGAGCACG
S2	PCR	Reverse	*S. cerevisiae HAC1* (2nd exon)	TGAAGTGATGAAGAAATCATTCAATTC
P7	qPCR	Forward	*KAR2*	TGCTTGGTAAATTCGAGCTG
P8	qPCR	Reverse	*KAR2*	CAACTTGAGGAGTACCTCTTGGA
P9	qPCR	Forward	*PDI1*	GGAAAGGCCCACGATGAAGTTGTC
P10	qPCR	Reverse	*PDI1*	GCATCCTCATCATTGGCGTAAAGAGTAG
P11	qPCR	Forward	*FES1*	CTCAGGATGAGGAATCCAAGA
P12	qPCR	Reverse	*FES1*	GGGCCTCCAAACAACTGAG
P13	qPCR	Forward	*YDJ1*	GACAAATTGGCCCCATGAT
P14	qPCR	Reverse	*YDJ1*	CTTCTCCGTTACAAACATCACATC

Table 6: Oligonucleotide primers used for RT-PCR and RT-qPCR analyses

High-throughput RNA-seq analysis was done in GenomeRead Co., Ltd. (Takamatsu, Japan). First, mRNA was purified from the total mRNA samples using the KAPA mRNA capture kit (KAPA Biosystems, Potters Bar, UK). Second, libraries were generated using the MGI Easy RNA directional library prep set (MGI Tech, Shenzhen, China), and were analyzed by the DNBSEQ-G400RS DNA sequencer (MGI Tech, Shenzhen, China; 2x150 bp paired-end reads, 1 Gb data/sample). Raw FASTAQ data were processed in the CLC Genomics Workbench (Qiagen, Venlo, Nederland). Reference data for gene mapping and gene annotation were obtained from Pichiagenome.org (http://pichiagenome-ext.boku.ac.at).

A first exon fragment of the *P. pastoris HAC1* gene was PCR amplified from CBS7473 genomic DNA using the primer set P31/P32 (GAGCAAAGACGGAAGAAGAAAAGG,CGGATGACAAAGGAGATGGAAGTTC) and was ^{32}P-radiolabeled with the Random Primer DNA Labeling Kit Ver.2 (Takara) for Northern-blot analysis using the procedure described by Ref. [14].

2.6 Protein analyses

After harvested by centrifugation at 1,600 × g for 1 min, 1.0=OD_{600} cells were disrupted by agitation with glass beads (425–600 μm) in 100 μL of the lysis buffer containing 50 mM Tris-Cl (pH7.9), 5 mM EDTA, 1% Triton X-100 and protease inhibitors (2 mM phenylmethylsulfonyl fluoride, 100 μg/ml leupeptin, 100 μg/ml aprotinin, 20 μg/ml pepstatin A, and Calbiochem Protease Inhibitor cocktail Set III (X100 dilution)), and were clarified by flash centrifugation at 750 × g for 30 sec. Protein concentration in the crude lysates was determined using BioRad Protein assay kit (Hercules, CA, USA) and was adjusted to 2.5 mg/ml by adding the lysis buffer. Subsequently, the crude lysates were further centrifuged at 8,400 × g for 20 min, and the pellet fractions were washed twice with the lysis buffer supplemented with 2 % NP-40.

Protein samples were fractionated by the standard Laemmli SDS-polyacrylamide gel electrophoresis as described previously [37], and the resulting gels were silver stained (Silver stain KANTO III; Kanto Chemical, Tokyo, Japan). Alternatively, the gels were subjected to Western-blot analysis as described previously [37]. The primary antibody used was Anti-GFP and Anti-ubiquitin from MBL (Woburn, U.S.A).

2.7 ^{35}S radio-labelling assay

P. pastoris cells were grown in SC medium [71] not containing methionine and cysteine. After pre-culturing at 30 °C, cells were continuingly incubated at 30 °C or shifted to 39 °C for 60 min. I then added 1 µL [^{35}S]-protein labelling mixture (PerkinElmer) to 10 mL cultures, which were further incubated for 10 min. Then, cell lysates were prepared as aforementioned.

2.8 Statistics

In order to perform statistical analyses, we generated three independent clones having the same genotype. The values are presented as averages and standard deviations from three biological replicates. To obtain *p* values, we performed two-tail unpaired t-test using Microsoft Excel. Alternatively, the RNA-seq data were processed by the CLC Genomics Workbench (Qiagen, Venlo, Nederland).

CHAPTER III: RESULTS

3.1 *HAC1*-mRNA splicing in *P. pastoris* cells is only partially reliant on external ER-stressing stimuli.

As described in the Introduction section, the *HAC1*-mRNA splicing profile in *P. pastoris* cells have not been well determined. At the beginning of this study, I therefore inquired scenes in which the *HAC1* mRNA is spliced in *P. pastoris* cells. In the experiment shown in Fig. 4A, the laboratory standard *P. pastoris* and *S. cerevisiae* strains CBS7435 and BY4742 were aerobically cultured at 30 ˚C in YPD medium under non-stress conditions or ER-stressed by the potent disulfide-bond reducing reagent dithiothreitol (DTT). Then, their total RNA samples were subjected to the RT-PCR analysis to monitor the *HAC1*-mRNA splicing. As widely known, the *HAC1*-mRNA splicing was strictly dependent on ER stress in *S. cerevisiae* cells (Fig. 4A). However, in the case of *P. pastoris* cells, the *HAC1* mRNA was considerably spliced even under non-stressed conditions, while the DTT treatment enhanced it (Fig. 4A).

In order to confirm the RT-PCR result, I next monitored the *HAC1*-mRNA splicing using another method. In the experiment shown in Fig. 4B, total RNA samples were subjected to the Northern-blot analysis, which exhibited a similar result as that shown by the RT-PCR analysis.

I next cultured *P. pastoris* cells in SD medium, which, as well as YPD, is a commonly used yeast medium. Although the optimum growth temperature of *P. pastoris* cells is around 30˚C, they are often cultured at lower temperatures (e.g., 25˚C) when applied for recombinant protein production [72, 73]. I therefore cultured *P. pastoris* cells not only at 30˚C but also at lower temperatures of 25 and 20 °C. As shown in Fig. 4C, unstressed *P. pastoris* cells exhibited a partial but considerable *HAC1*-mRNA splicing, which was enhanced by treatment of cells with DTT.

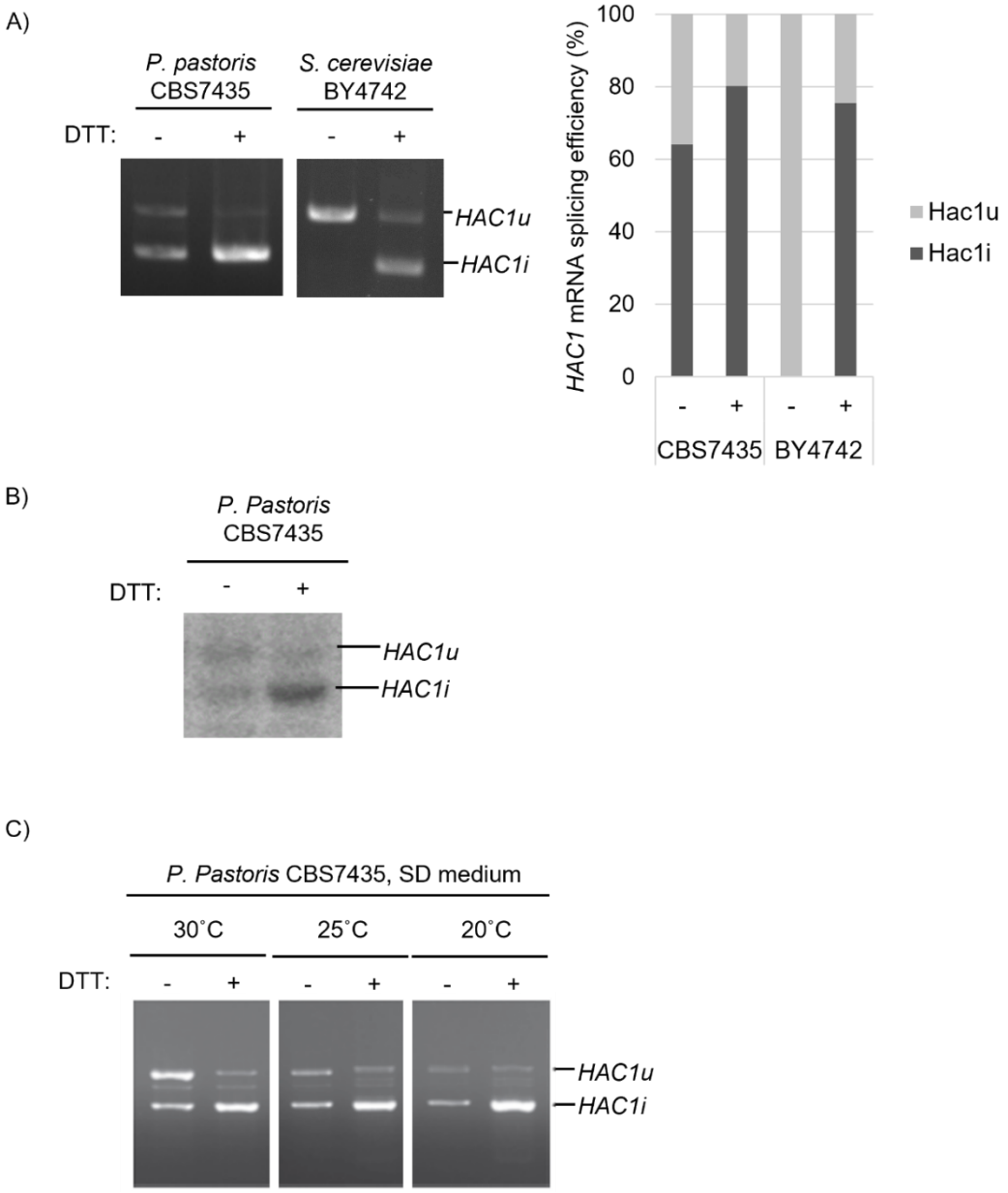

Figure 4: The *HAC1*-mRNA splicing in the *P. pastoris* and *S. cerevisiae* cells. Yeast cells were cultured at 30 °C in YPD (A, B) or at the indicated temperatures in SD (C). For the DTT (+) sample, I added 10 mM (final conc.) DTT into cultures, which were further shaken for 30 min. To detect the *HAC1*-mRNA species, total RNA samples were subjected to the RT-PCR (A and C) or Northern-blot analyses (B).

3.2 *S. cerevisiae* Ire1 is tightly regulated even when carrying the luminal domain of *P. pastoris* Ire1.

As a possible reason for the considerable *HAC1*-mRNA splicing in unstressed *P. pastoris* cells, I hypothesized that as an intrinsic nature, *P. pastoris* Ire1 is controlled more loosely than *S. cerevisiae* Ire1.

Ire1 is composed of the ER luminal domain, which acts as a stress-sensing regulatory region, and the cytosolic domain, which acts as an effector region. The luminal domain detects ER-accumulated misfolded proteins and promotes oligomerization and activation of the cytosolic domain, which catalyses the splicing of *HAC1*-mRNA [74]. As shown in Fig. 5A, I therefore constructed a chimeric mutant gene of *S. cerevisiae* Ire1 carrying the luminal domain of *P. pastoris* Ire1 and expressed it in *S. cerevisiae* cells.

Fig. 5B shows that the *HAC1*-mRNA splicing was provoked only upon ER stress in *S. cerevisiae* cells producing the chimeric Ire1 version as well as those producing wild-type Ire1. This observation suggests that contrary to the aforementioned hypothesis, both the luminal domain of *P. pastoris* Ire1 and *S. cerevisiae* Ire1 have an inherent ability to activate Ire1 solely in response to ER stress. As described in the Discussion section, I now deduce that in *P. pastoris* cells, protein secretion is robust enough to lead to the ER-stress induction and the *HAC1*-mRNA splicing even without external stressing stimuli.

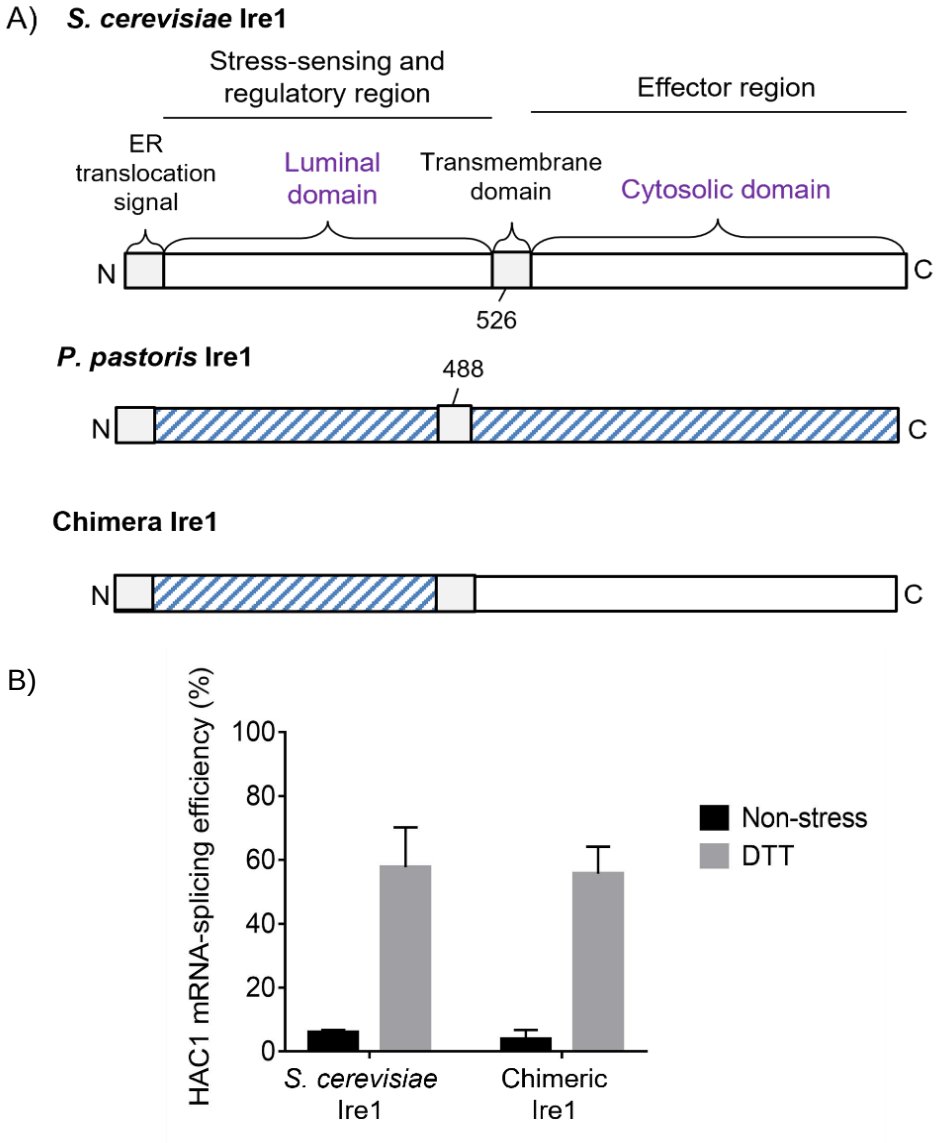

Figure 5: DTT-dependent regulation of the *P. pastoris/S. cerevisiae* chimeric Ire1 mutant. *S. cerevisiae ire1Δ* strain KMY1516 were transformed with pRS313-IRE1, which is a single copy YCp plasmid carrying the authentic *S. cerevisiae IRE1* gene or its chimeric mutant version. (A) Structure of the Ire1 chimeric mutant. (B) The transformants were exponentially grown at 30˚C in SD under non-stress conditions or stressed by 5 mM DTT for 1 hr before monitoring the *HAC1*-mRNA splicing.

3.3 The *IRE1* knockout mutation (*ire1Δ*) but not the *HAC1* knockout mutation (*hac1Δ*) induced heat shock target genes in *P. pastoris* cells.

In order to further elucidate the UPR signalling pathway in *P. pastoris* cells, I next knocked out two master regulator genes of the UPR, *IRE1* and *HAC1*. As described in the Materials and Methods section, the *IRE1* knockout mutation (*ire1Δ*), which was designated as the *ire1Δ0* allele, was accomplished using the CRISPR/Cas9 technology, resulting in the deletion of the full-length *IRE1* gene (Fig. 6A). The *HAC1* knockout mutation (*hac1Δ*), which was designated as the *hac1::KanMX* allele, was achieved by replacement of the genomic *HAC1* gene to a G418-resistant *KanMX* marker, resulting in deletion of the full-length *HAC1* gene (Fig. 6B).

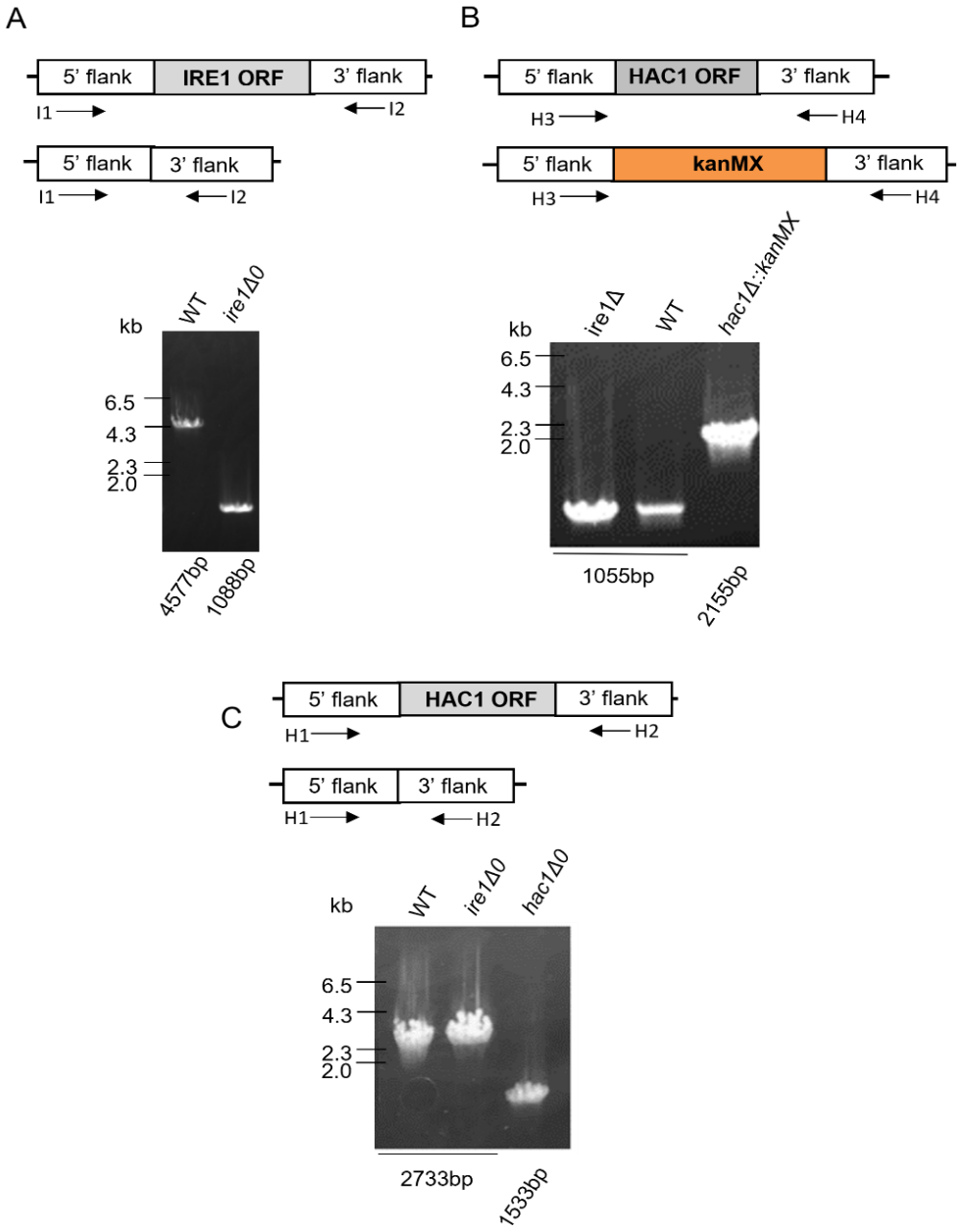

Figure 6: Construction of *P. pastoris IRE1* or *HAC1* knockout mutants. The genomic mutations on the *P. pastoris* wild-type (WT) strain CBS7435 were confirmed through PCR using the genomic DNA samples and the indicated oligonucleotide primers (I1, I2, H1, H2, H3, or H4), which was followed by agarose-gel electrophoresis. The fluorescent images of EtBr-stained gels are shown.

In the experiment shown in Fig. 7A, I detected the *HAC1* mRNA species in unstressed *P. pastoris* cells using the RT-PCR technique. As expected, the *HAC1* mRNA was not spliced in *ire1Δ0* cells, and it was not detected in *hac1::KanMX* cells. I then performed quantitative analysis by RT-qPCR analysis, which revealed that the *HAC1* gene is downregulated in *ire1Δ0* cells (Fig.7A- right panel). This result is consistent with the RNA-seq data shown later.

KAR2 and *PDI1*, both of which encode essential factors involved in protein folding in the ER, are prominent UPR target genes in *S. cerevisiae*. According to the previous report by others [62], [64], these genes are induced by the UPR also in *P. pastoris* cells. I therefore monitored their expression profile using the RT-qPCR technique. The *PDI* expression profile was consistent with the notion that both *IRE1* and *HAC1* are inevitable to the UPR and work exactly on the same pathway. DTT caused a substantial induction of the *PDI1* expression, which was equally abolished by the *ire1Δ0* or *hac1::KanMX* mutation (Fig. 7B). As shown in (Fig. 7C), expression of *KAR2* was also induced by DTT in wild-type cells and compromised by the *ire1Δ0* or *hac1::KanMX* mutation. However, unexpectedly, the *KAR2* expression was somewhat higher in *ire1Δ0* cells than *hac1::KanMX* cells both under non-stress and DTT-stress conditions (Fig. 7C).

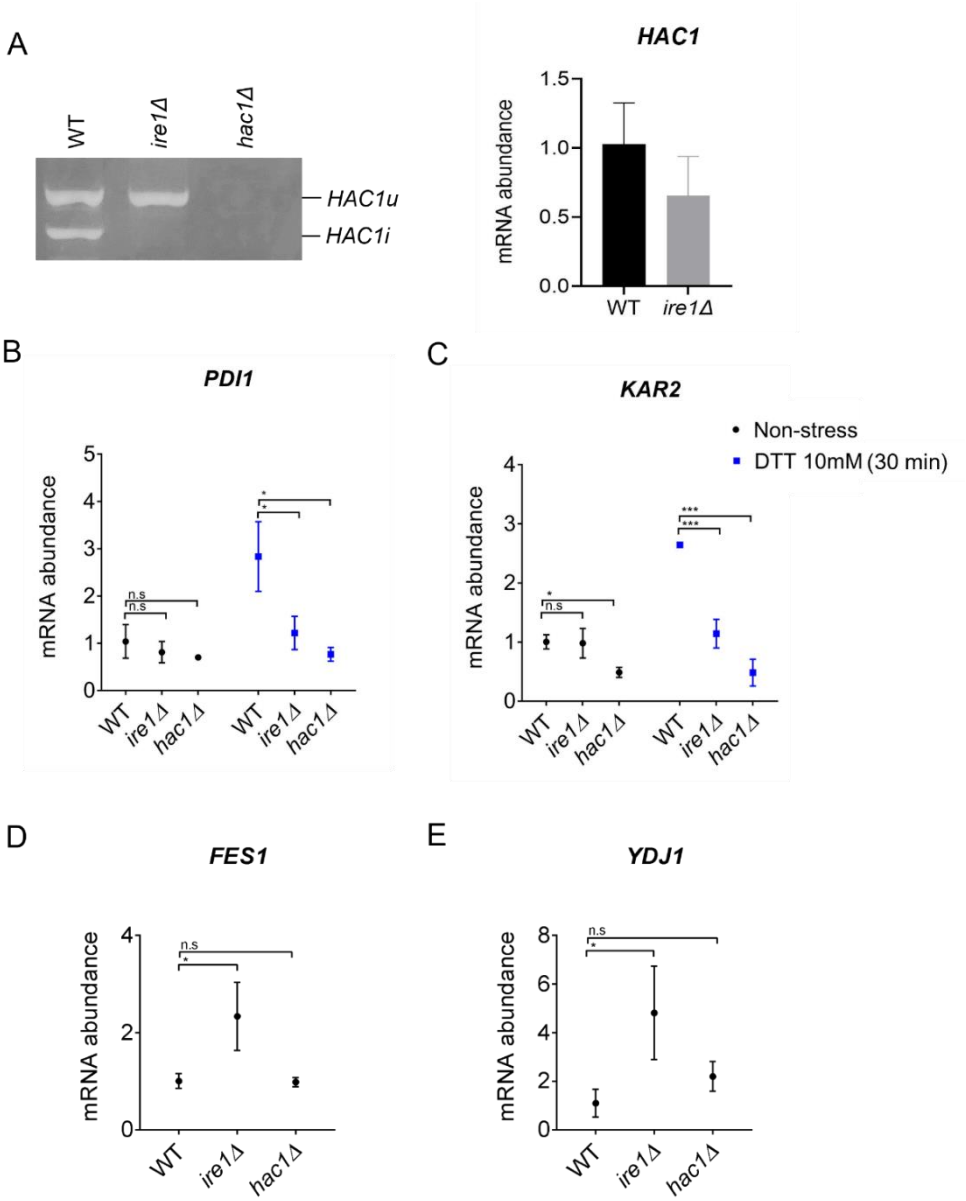

Figure 7: Expression profile of UPR- and HSR-target genes in *P. pastoris* cells carrying the *ire1Δ0* or *hac1::kanMX* mutations. *P. pastoris* wild-type cells (WT; CBS7435) and its *ire1Δ0* or *hac1::kanMX* mutants were cultured in YPD at 30°C. For the DTT(+) sample, I added 10 mM (final conc.) DTT into cultures, which were further shaken for 30 min. The total RNA samples were analysed by RT-PCR followed by agarose-gel electrophoresis and EtBr staining (A left panel; *HAC1*) or RT-qPCR (A; right panel-E). The result values are presented as relative to those of non-stressed WT cells, which are set at 1.0. n.s: not significant, * $p<0.05$, *** $p<0.001$.

In order to confirm this result, I constructed another allele of the *hac1Δ* mutation, namely *hac1Δ0*, using the CRISPR/Cas9 technology (Fig. 6C). The *ire1Δ0hac1Δ0* double deletion mutant was also created. In the experiment shown in Fig. 8, I cultured the resulting strains under non-stress conditions and checked the *PDI1* and *KAR2* expression levels using the RT-qPCR technique. As shown in Fig. 8A, the *ire1Δ0* and *hac1Δ0* mutations (and the *ire1Δ0hac1Δ0* double mutation) almost equally and slightly decreased the *PDI1* expression level. This observation is consistent with the aforementioned insight that in *P. pastoris* cells, the UPR is induced even under non-stress conditions albeit weakly. On the contrary, the expression level of the *KAR2* gene was significantly decreased by the *hac1Δ0* mutation but not by the *ire1Δ0* mutation or the *ire1Δ0hac1Δ0* mutation (Fig. 8B)

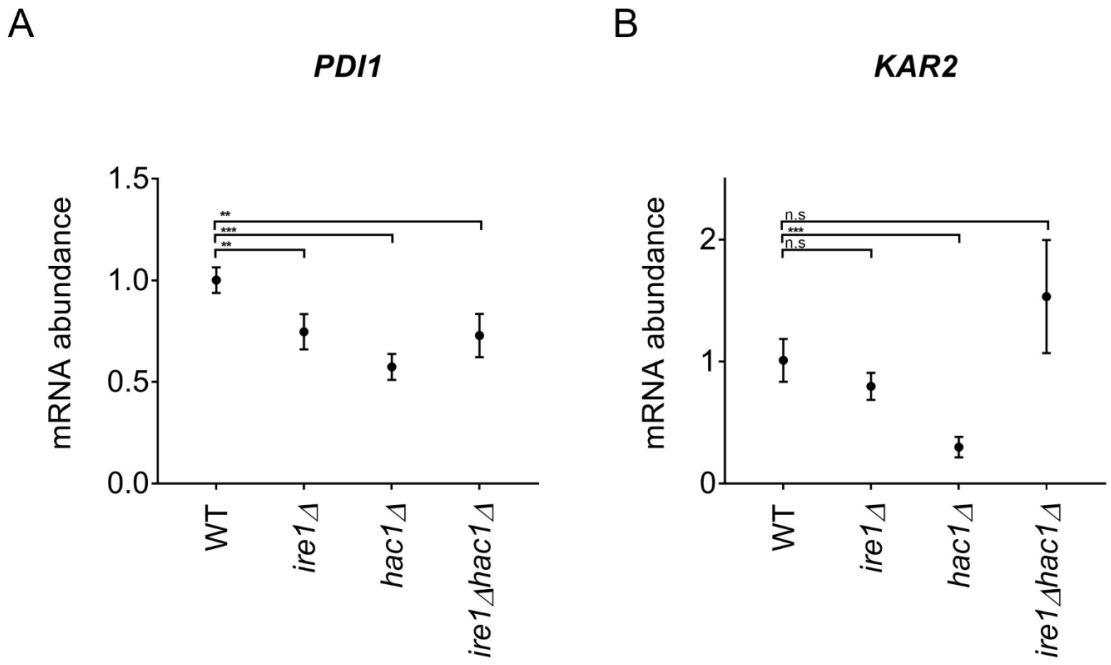

Figure 8: Expression profile of UPR-target genes in *P. pastoris* cells carrying the *ire1Δ0* and/or *hac1Δ0* mutations. *P. pastoris* wild-type cells (WT; CBS7435) and its mutants carrying the *ire1Δ0* and/or *hac1Δ0* mutations were cultured in YPD at 30°C. The RNA samples were analysed by RT-qPCR, and the result values are presented as relative to that of WT cells, which are set at 1.0. n.s.: not significant, **: $p<0.01$, ***: $p<0.001$, ****: $p<0.0001$.

I therefore deduce the following scenario. As well as in *S. cerevisiae* cells, the UPR is dependent on both *IRE1* and *HAC1* in *P. pastoris* cells. While the *PDI1* expression is controlled solely by the UPR, which, however, is not the sole determinant to control the *KAR2* expression level. In other words, the *ire1Δ* mutation affects the *KAR2* expression level via two different ways. First, the *ire1Δ* mutation, as well the *hac1Δ* mutation, abolishes the UPR, leading to reduction of the *KAR2* expression level. However, the *ire1Δ* mutation also induces the *KAR2* expression independently of *HAC1*.

According to Ref. [75], *KAR2* is transcriptionally induced not only by the UPR but also by the heat shock response (HSR) in *S. cerevisiae* cells. The promoter region of the *S. cerevisiae KAR2* gene carries two different elements respectively responsive responsible for the transcriptional induction upon the UPR and the HSR. Thus, I inferred that under non-stress conditions, the *ire1Δ* mutation, but not the *hac1Δ* mutation, induces the HSR, leading to higher *KAR2* expression in *ire1Δ* cells than in *hac1Δ* cells. The HSR is known to cause the transcriptional induction of genes encoding molecular chaperones and chaperone co-factors working in the cytosol and/or nucleus

[76]. Therefore, in order to check my hypothesis, I examined the expression level of two HSR markers, *FES1* and *YDJ1*, which encode cytosolic Hsp70 co-factors and are known to be induced by heat shock in other species [73-75]. Strikingly, as shown in Figs. 7D and E, the *ire1Δ0* mutation, but not the *hac1::KanMX* mutation, significantly increased the expression of *FES1* and *YDJ1* under non-stress.

My findings concerning the *ire1Δ* mutation were confirmed using another *ire1Δ* allele, *ire1::kanMX*, which had been created through insertion of the G418-resistant marker into the *IRE1* gene. As expected, the *ire1::kanMX* mutation compromised the *PDI1* expression and increased the *FES1* and *YDJ1* expression (Fig. 9). Considering also the phenotypic resemblance between the *hac1::kanMX* mutation and the *hac1Δ0* mutation (Figs. 7 and 8), I deduce that my observations described so far are not due to off-target mutations of genes other than *IRE1* and *HAC1*.

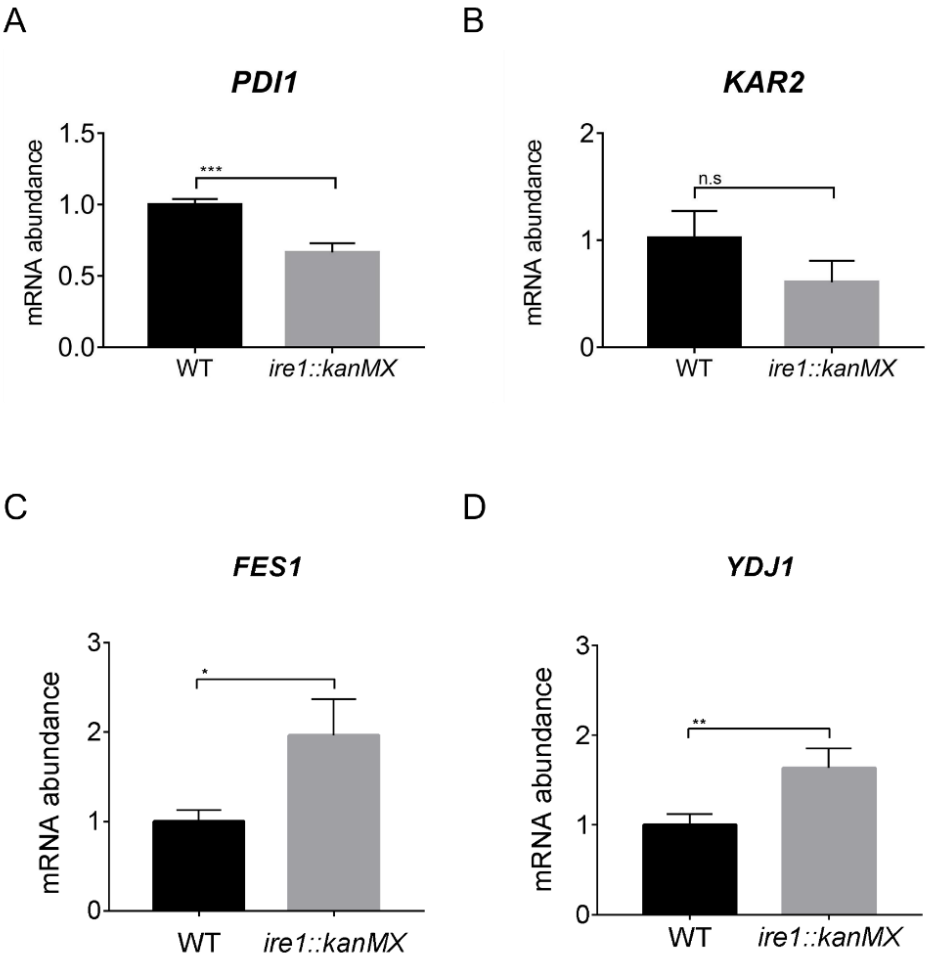

Figure 9: Expression profile of UPR- and HSR-target genes in *P. pastoris* cells carrying the *ire1::kanMX* mutations. *P. pastoris* wild-type cells (WT; CBS7435) and its mutant carrying the *ire1::KanMX* mutation were cultured in YPD at 30°C. The RNA samples were analysed by RT-qPCR, and the result values are presented as relative to that of WT cells, which are set at 1.0. n.s; not significant, *: $p<0.05$, **: $p<0.002$, *** $p<0.001$.

3.4 Global gene expression alteration by the *ire1Δ* and/or *hac1Δ* mutations in *P. pastoris* cells.

In order to further understand the phenotypic difference between the *ire1Δ* and *hac1Δ* mutations, I next performed transcriptome analysis of *P. pastoris* cells using the mRNA-seq technique. I employed cells carrying the *ire1Δ*0 and/or *hac1Δ*0 mutations, which hereafter called simply the *ire1Δ* and/or *hac1Δ* mutations, but not the *ire1::kanMX* or *hac1::kanMX* mutants, because the highly expressed heterologous drug-resistance marker may affect the transcriptome. Because as aforementioned, the *IRE1/HAC1*-dependent UPR system is activated even without external stress stimuli, although not very strongly, in *P. pastoris* cells., I obtained RNA samples from unstressed cells

The comprehensive result of the mRNA-seq analysis of unstressed wild-type, *ire1Δ, hac1Δ*, and *ire1Δhac1Δ* cells are listed in Table S1 and illustrated by volcano plots presented in Figs. 10A-E. It should be noted that the expression level of *HAC1* was positively and significantly regulated by *IRE1* (Fig. 10A, 7A- right panel). This is presumably because the *HAC1* gene is transcriptionally upregulated by the Hac1 protein, which is the translation product of the *HAC1*i mRNA. As described in the Introduction section, a similar phenomenon was previously reported in an *S. cerevisiae* study [28] and is likely to contribute to a sustained induction of the UPR.

Interestingly, the *ire1Δhac1Δ* vs *hac1Δ* and *ire1Δhac1Δ* vs *ire1Δ* comparisons (Figs. 10D and E) revealed a number of differentially expressed genes (DEGs), indicating that *IRE1* and *HAC1* may act through different pathways in *P. pastoris*. This idea is supported by the Venn diagrams shown in Fig. 11A, which indicate that the DEGs of the *ire1Δ* mutation (*ire1Δ* vs. WT comparison) and those of the *hac1Δ* mutation (*hac1Δ* vs. WT comparison) did not overlap perfectly. Moreover, the DEGs in the *hac1Δ* vs. WT and *ire1Δhac1Δ* vs. *hac1Δ* comparisons overlapped only slightly (eleven induced and two repressed DEGs), supporting our proposal that the *HAC1*-dependent and the *HAC1*-independent functions of *IRE1* are distinct (Fig. 11B).

Fig. 12 shows that the aforementioned observations obtained through the RT-qPCR analyses (Figs 7 and 8) were reproduced in the mRNA-seq analysis.

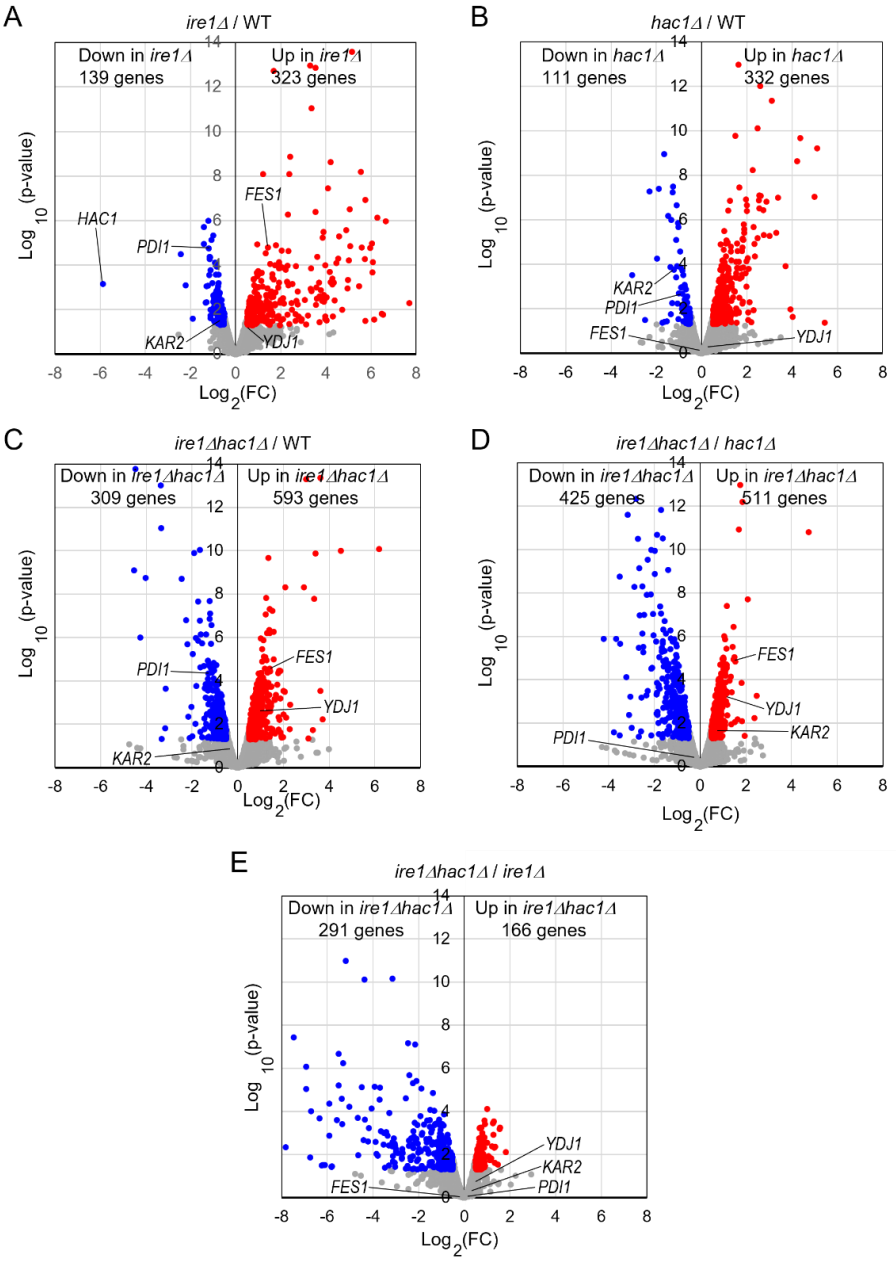

Figure 10: Volcano plot produced by transcriptome analysis of *P. pastoris* cells carrying the *ire1Δ* and/or *hac1Δ* mutations. *P. pastoris* wild-type cells (WT; CBS7435) and its mutants carrying the *ire1Δ0* and/or *hac1Δ0* mutations were cultured in YPD at 30°C. The RNA samples were then subjected the mRNA-seq analysis, and the result is presented as the volcano plots (A-E). DEGs ($p<0.05$; $Log_2(FC)<-0.5$ or >0.5) are colored. FC: Fold change.

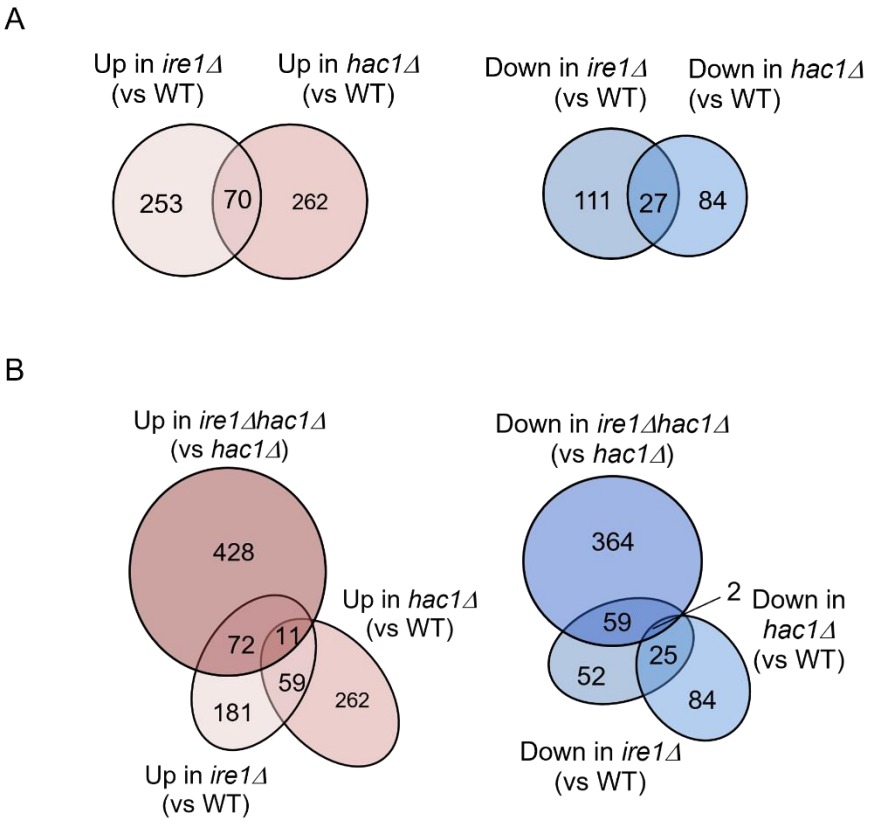

Figure 11: Venn diagram produced by transcriptome analysis of *P. pastoris* cells carrying the *ire1Δ* and/or *hac1Δ* mutations. *P. pastoris* wild-type cells (WT; CBS7435) and its mutants carrying the *ire1Δ0* and/or *hac1Δ0* mutations were cultured in YPD at 30°C. The RNA samples were then subjected the mRNA-seq analysis, and the result is presented as the Venn diagrams. (A) DEGs compared to WT and (B) combination of (A) with *ire1Δ0hac1Δ0*/ *hac1Δ0* mutant. DEGs ($p<0.05$; $Log_2(FC)<-0.5$ or >0.5) are counted. FC: Fold change.

Heat Map of genes encoding UPR and HSR target genes

	log_2(fold change TPM) = log_2 (below)			
	ire1△/WT	*hac1△*/WT	*ire1△hac1△*/ WT	*ire1△hac1△*/ *hac1△*
PDI1	-1.19*	-0.85*	-1.14*	-0.28
KAR2	-0.68*	-1.22*	-0.46	0.76*
FES1	1.43*	-0.07	1.39*	1.46*
YDJ1	0.54	-0.14	0.94*	1.09*

* : p-value (<0.05)

Figure 12: Expression profiles of the UPR and HSR marker genes determined by the mRNA-seq analysis. Form the result of the mRNA-seq analysis presented in Fig. 10 and Table S1, that of four selected genes are extracted and presented as a heat map. *: $p<0.05$, FC: Fold change.

3.5 *P. pastoris* Ire1 has various potential targets.

Next, I screened the total mRNA-seq data (Fig. 10 and Table S1) for DEGs cooperatively induced by *IRE1* and *HAC1* (Category A) and controlled only by *IRE1* (Category B or C) as illustrated in Fig. 13. Using the screening criteria presented in Fig. 14, we selected 15 named genes as the Category-A DEGs (Table S2). Fig. 14 also shows the heat-map expression data of the named genes belonging to Category A. Consistent with our expectation that the Category-A genes are targets of the traditional UPR, many of them are known to be involved in ER protein translocation, folding, and modification (see the Discussion section for details).

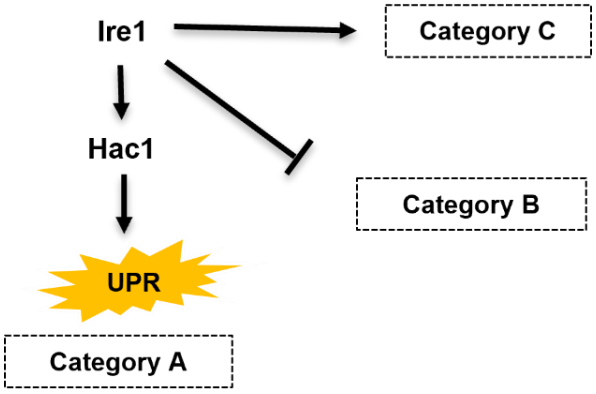

Figure 13: Categorisation of the *Pichia* Ire1-target genes.

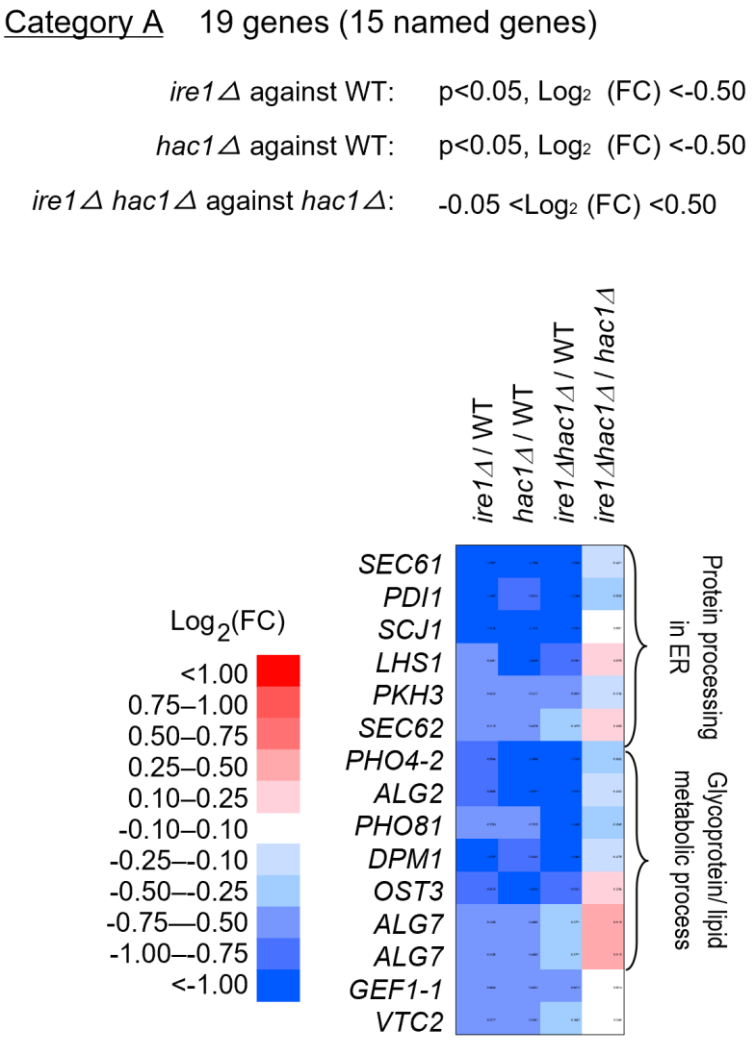

Figure 14: Genes cooperatively induced by *IRE1* and *HAC1*. The mRNA-seq data shown in Table S1 and Fig. 10 were screened using the indicated criteria to extract the DEGs belonging to Category A. The heat map presents the expression profile of the named genes belonging to Category A. FC: Fold change.

Category B is a group of genes that were repressed by *IRE1* independent of *HAC1* (Fig. 15 and Table S2). The screening criteria for Category B are DEGs with elevated expression in comparison of *ire1Δhac1Δ* cells against *hac1Δ* cells. As shown in Fig. 15, many of the Category-B genes were induced in ire1*Δ* cells and *ire1Δhac1Δ* cells compared to wild-type cells. As expected from our observations from the RT-qPCR analysis (Figs. 7-9), *KAR2*, *YDJ1* and *FES1* fell into Category B. Expression of *FES1* and *YDJ1* was high in *ire1Δ* and *ire1Δhac1Δ* cells (Figs. 12 and 15). Moreover, the expression of *KAR2* was considerably lowest in *hac1Δ* cells (Figs. 12 and 15), presumably because it was induced by the HSR in *ire1Δ* and *ire1Δhac1Δ* cells.

Table 7 shows that in the KEGG pathway database, genes encoding ribosomal proteins and those related to ribosome biogenesis were highly enriched in Category B. It should also be noted that many genes related to the proteasome and ubiquitylation fell into Category B (Fig. 15 and Table 7).

Category C is a group of genes induced by *IRE1* independent of *HAC1* (Fig. 16 and Table S2). As shown in Table 8, genes for glycolysis/gluconeogenesis and various metabolic pathways were highly enriched in Category C.

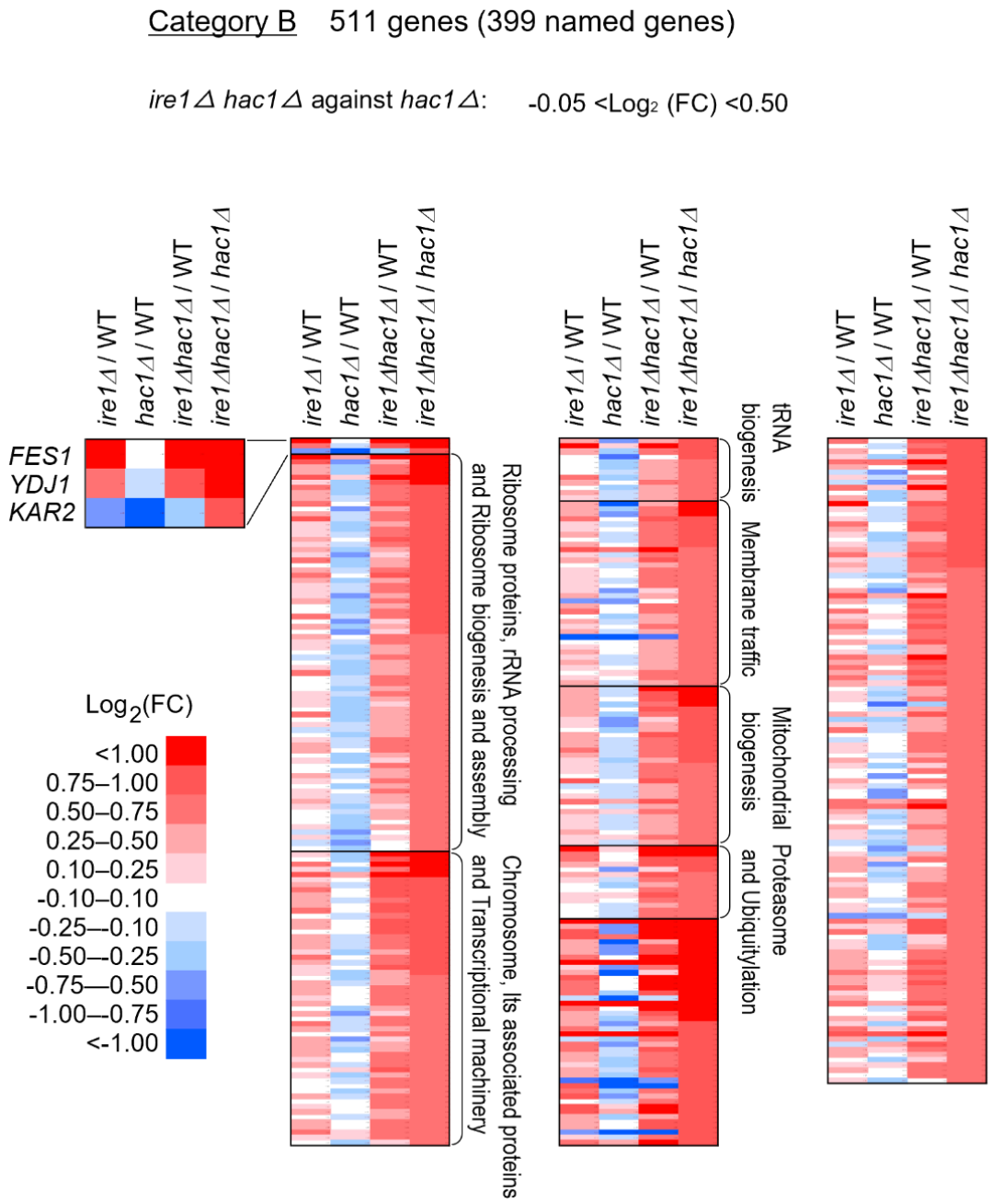

Figure 15: Genes suppressed by *IRE1* independently of *HAC1*. The mRNA-seq data shown in Table S1 and Fig. 10 were screened using the indicated criteria to extract DEGs belonging to Category B. The heat map presents the expression profiles of the named genes in Category B, which are listed in Table S2. FC: Fold change.

Category B	
Pathway name	p-value
Ribosome	9.278e-9
Ribosome biogenesis in eukaryotes	2.837e-8
Nucleotide excision repair	0.000007329
Basal transcription factors	0.00003546
Protein processing in endoplasmic reticulum	0.00006509
Proteasome	0.00006038
DNA replication	0.0003414
Autophagy	0.0002949
mRNA surveillance pathway	0.0002897
Folate biosynthesis	0.0008520

Table 7: KEGG pathway enrichment of the Category-B genes. Lists of named genes were inputted to the YeastEnrichr WEB site, and the results of the data analysis (KEGG 2019 pathways) are indicated.

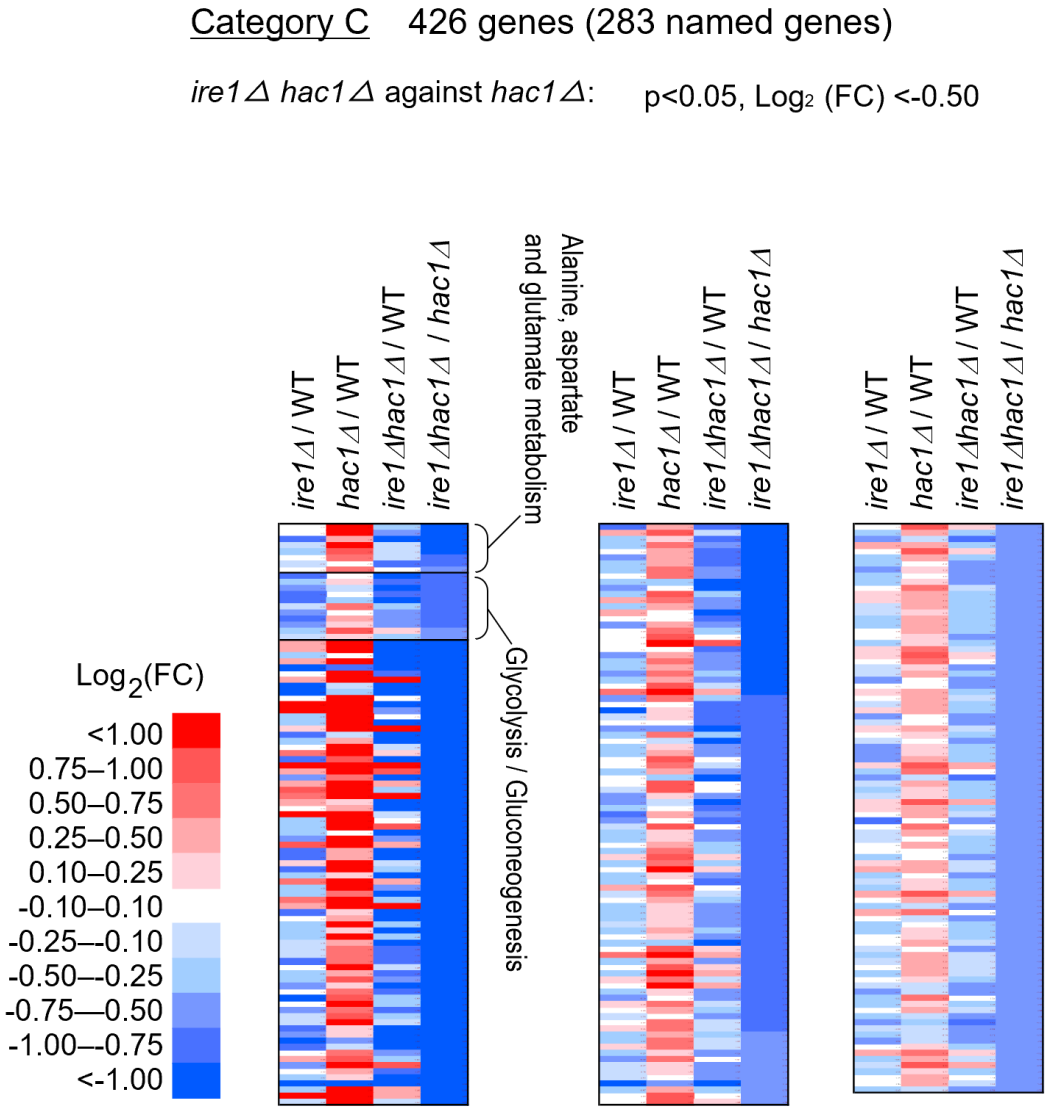

Figure 16: Genes induced by *IRE1* independently of *HAC1*. The mRNA-seq data shown in Table S1 and Fig. 10 were screened using the indicated criteria to extract DEGs belonging to Category C. The heat map presents the expression profiles of the named genes in Category C, which are listed in Table S2. FC: Fold change.

Category C	
Pathway name	p-value
Glycolysis / Gluconeogenesis	2.016e-10
Alanine, aspartate and glutamate metabolism	8.425e-9
Starch and sucrose metabolism	5.959e-8
Nitrogen metabolism	5.677e-7
Fructose and mannose metabolism	3.384e-7
Methane metabolism	0.000001053
Steroid biosynthesis	0.000002897
Sphingolipid metabolism	0.00003465
MAPK signaling pathway	0.000004962
Arginine biosynthesis	0.00007968

Table 8: KEGG pathway enrichment of the Category-C genes. Lists of named genes were inputted to the YeastEnrichr WEB site, and the results of the data analysis (KEGG 2019 pathways) are indicated.

3.6 The *ire1Δ* mutation causes aggregation of proteins in *P. pastoris* cells.

As aforementioned, the *ire1Δ* mutation, but not the *hac1Δ* mutation, induced the HSR in *P. pastoris* cells. It is widely accepted that the HSR is a cellular protective response that is activated alongside aggregation of proteins in the cytosol and/or nuclei [77]. For instance, an artificially expressed misfolded protein, namely expanded polyQ bodies, induces the HSR in *S. cerevisiae* cells albeit weakly [78]. Misfolded proteins are associated with the HSP70-family molecular chaperones, which are then incapable of downregulating the transcription factor Hsf1 that is responsible for the HSR [79].

Therefore, I examined protein aggregation in *P. pastoris* by performing a protein-aggregation analysis. In the experiment shown in Fig. 17, cells were cultured under non-stress conditions, and their lysates were fractionated by centrifugation. Fig. 17A indicates that the pellet fractions of *ire1Δ* cells and *ire1Δhac1Δ* cells contained more abundant proteins than those of WT or *hac1Δ* cells. Anti-ubiquitin Western blot analysis showed that proteins in the pellet fractions were ubiquitylated, at least partly (Fig. 17B).

These observations strongly suggest a role of *IRE1* to prevent protein aggregation in the nuclei/cytosol.

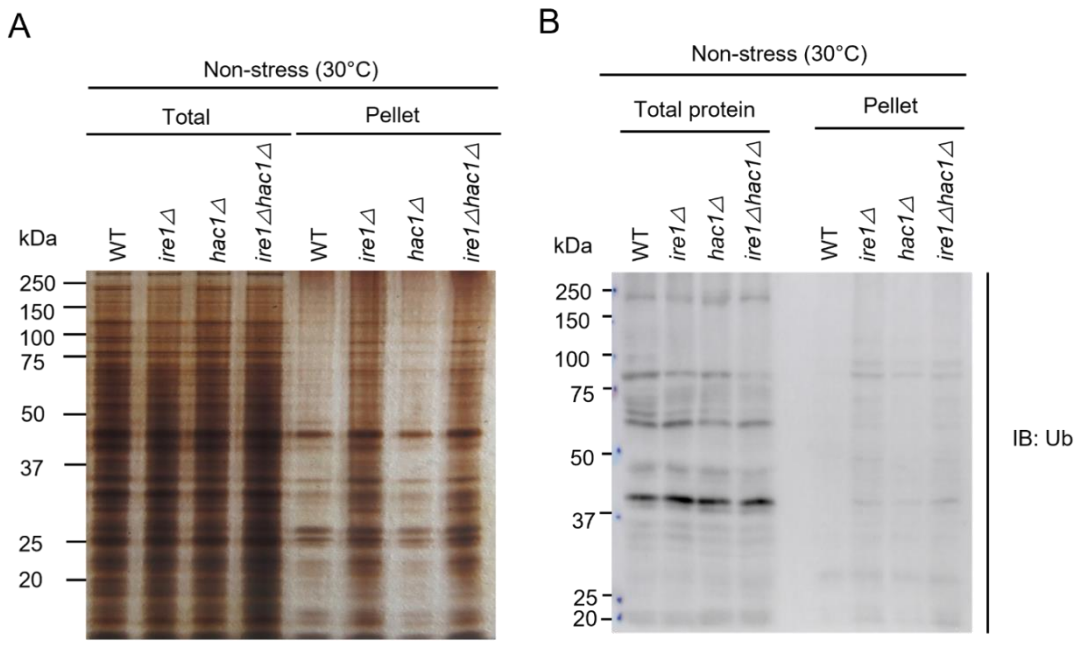

Figure 17: Induction of protein aggregation by the *ire1Δ* mutation. After culturing at 30 °C under non-stress conditions, *P. pastoris* wild-type cells (WT; CBS7435) and its mutants carrying the *ire1Δ0* and/or *hac1Δ0* mutations were harvested and lysed. The crude lysates (Total) were then subjected to high-speed centrifugation, and the pellet fractions (Pellet) were obtained. Protein samples (Total: crude lysates corresponding to 6 µg protein; Pellet: preparation from crude lysates corresponding to 16 µg protein) were separated by SDS-PAGE, and the resulting gels were subjected to the silver staining (A) or anti-ubiquitin (Ub) immunoblotting (B).

3.7 Growth properties of *P. pastoris* cells carrying the *ire1Δ* and/or *hac1Δ* mutations.

I next monitored growth of *P. pastoris* wild-type and mutant cells in liquid YPD medium cultured at 30 °C. As shown in Fig. 18, growth was retarded when the *ire1Δ* or *hac1Δ* mutation was introduced. It should be also noted that the *ire1Δhac1Δ* double mutation exhibited more severe growth retardation than the single mutations (Fig. 18). This finding supports my argument that unlike the case of *S. cerevisiae* cells, *IRE1* and *HAC1* function on partly different pathways.

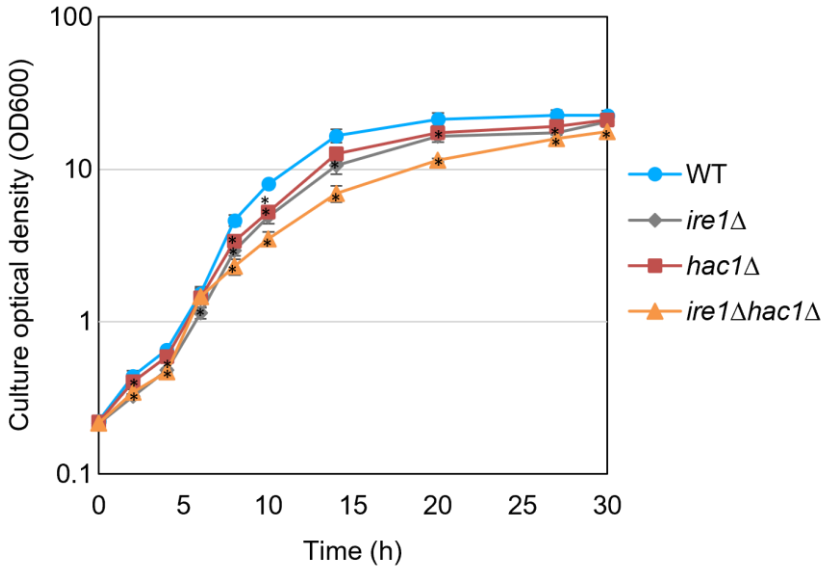

Figure 18: Growth profile of *P. pastoris* cells carrying the *ire1Δ* and/or *hac1Δ* mutations. After setting the initial OD_{600} values to approximately 0.3, the YPD cultures of *P. pastoris* wild-type cells (WT; CBS7435) and its mutants carrying the *ire1Δ0* and/or *hac1Δ0* mutations were aerobically shaken at 30 °C under non-stress conditions and monitored for the optical density. *: Significant change from WT ($p<0.05$).

Growth of *P. pastoris* cells were also checked by the spot growth assay on YPD agar plates (Fig. 19). In agreement with the aforementioned liquid growth assay (Fig. 18), the *ire1Δhac1Δ* strain seemed to grow more slowly than other strains (Fig. 19A). Tunicamycin is an N-glycosylation-inhibiting antibiotic that is frequently used as a potent ER stressor. *S. cerevisiae* cells carrying the *ire1Δ* or *hac1Δ* mutation is known to be hypersensitive to tunicamycin. Consistently, tunicamycin retarded the growth of cells carrying the *ire1Δ* and/or *hac1Δ* mutations more severely compared to that of wild-type cells also in the case of *P. pastoris* (Fig. 19B). Moreover, intriguingly, *hac1Δ* cells seemed to be more susceptible to tunicamycin than *ire1Δ* and *ire1Δhac1Δ* cells (Fig. 19B).

As aforementioned, a difference between *hac1Δ* cells and *ire1Δ* or *ire1Δhac1Δ* cells are that the HSR is provoked in the latter case. I therefore inquired what happen when the HSR is induced in *hac1Δ* cells by high-temperature (39 °C) treatment, which, as described later, triggers the HSR. In the experiment shown in Figs. 19C and D, cells were incubated at 39 °C for 60 min before being spotted onto agar plates. Strikingly, this heat shock treatment partly mitigated the severe sensitivity of *hac1Δ* cells to tunicamycin (compare Fig. 19D to B). Taken together, this is an intriguing case in which the impairment of the UPR is compensated by the HSR.

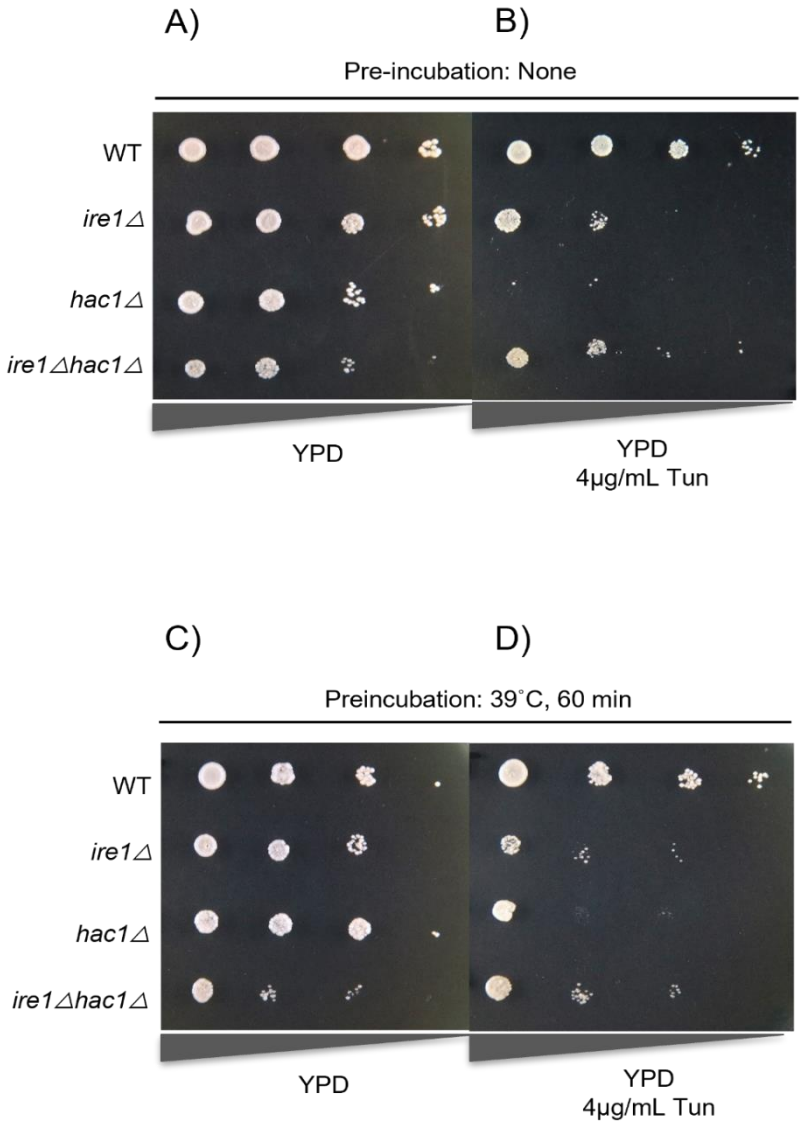

Figure 19: Tunicamycin sensitivity of *P. pastoris* cells carrying the *ire1Δ* and/or the *hac1Δ* mutations. Cultures (OD600=1.0) of *P. pastoris* wild-type cells (WT; CBS7435) and its mutants carrying the *ire1Δ0* and/or *hac1Δ0* mutations were 10-fold serially diluted and spotted onto YPD agar plates, which were incubated at 30 °C for 2 days before being photographed. In B and D, agar plates contained 4.0 μg/ml tunicamycin (Tun). In C and D, cultures were incubated at 39 °C for 60 min before spotting.

3.8 Involvement of *IRE1* and *HAC1* in properties of heat-shocked *P. pastoris* cells.

To elucidate the involvement of the UPR factors in the HSR more deeply, we examined the response of *P. pastoris* cells to high-temperature culturing. Fig. 20A shows that splicing of *HAC1* mRNA was induced by a temperature shift from 30 °C to 39 °C, indicating UPR induction upon this temperature shift. Consistent with our proposal that the *PDI* expression is positively regulated by the UPR but not by the HSR, it was induced by this temperature shift in wild-type cells but not in *ire1Δ* cells, *hac1Δ* cells, or *ire1Δhac1Δ* cells (Fig. 20B).

Moreover, as shown in Figs. 20D and E, this temperature shifts also elevated the expression of the HSR marker genes *FES1* and *YDJ1*. Because the temperature-dependent induction of these genes was stronger than that caused by the *ire1Δ* mutation at 30 °C (compare Figs. 20D and E to Figs. 7D and E), I deduced that the *ire1Δ* mutation alone only moderately induces the HSR. Figs. 20D and E also show that this temperature shift led to greater upregulation of the HSR marker genes in *ire1Δ* cells and *ire1Δ hac1Δ* cells than in WT cells or *hac1Δ* cells. Thus, we presume that the HSR was additively or cooperatively induced by the temperature shift and the *ireΔ* mutation. The expression pattern of *KAR2* (Fig. 20C) can be explained by our proposition that in *P. pastoris* cells, *KAR2* is dually regulated by the UPR and HSR.

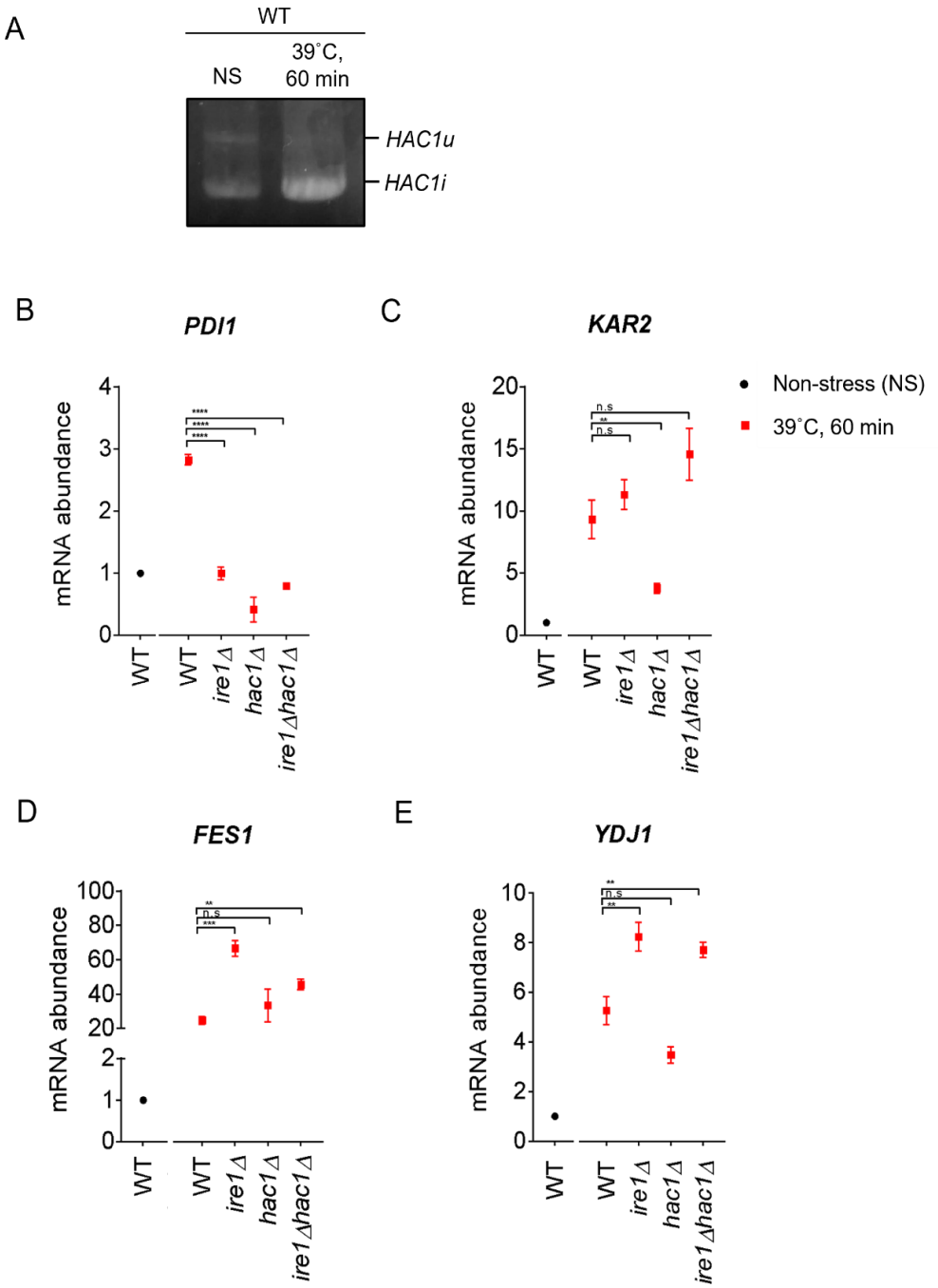

Figure 20: Heat shock-induced alteration of *HAC1* mRNA-splicing and gene-expression profiles of *P. pastoris* cells. *P. pastoris* wild-type cells (WT; CBS7435) and its mutants carrying the *ire1Δ0* and/or *hac1Δ0* mutations were cultured in YPD at 30°C (Non-stress; NS) or shifted to 39 °C for 60 min. (A) Total RNA samples were subjected to RT-PCR to amplify the *HAC1* cDNA variants, which were then fractionated by agarose gel electrophoresis. (B)-(E) Total RNA samples were subjected to RT-qPCR analysis using PCR primer sets that were specific to the indicated genes. Values are presented as relative to that of wild-type cells cultured at 30 °C, which is set at 1.0. n.s.: not significant, **: p<0.01, ***: p<0.001, ****: p<0.0001.

As aforementioned, the HSR is believed to be induced by accumulation of protein aggregates in the cytosol and/or nuclei. I therefore monitored aggregation of cytosolic and/or nuclear proteins using GFP as a model protein. In the experiment shown in Fig. 21, *P. pastoris* cells were transformed with a plasmid for expression of GFP from the strong and constitutive *GAP1* promoter. Subsequently, their lysates were separated by centrifugation as done in Fig. 17, and the total lysates and pellet fractions were analyzed by anti-GFP Western blotting.

As shown in in Figs. 21A, GFP was only slightly detectable in the pellet samples obtained from cells cultured at 30 °C. On the other hand, GFP came to the pellet fractions at least partly when cells were heat-shocked at 39 °C before cell lysis (Figs. 21A). It should be noted that the *ire1Δ* mutation, but not the *hac1Δ* mutation, seemed to aggravate the GFP aggregation (Figs. 21A). Fig. 21B is a control experiment that shows that no bands were observed from the lysate samples obtained from cells not containing the GFP gene, indicating that my anti-GFP Western blotting is actually specific to GFP.

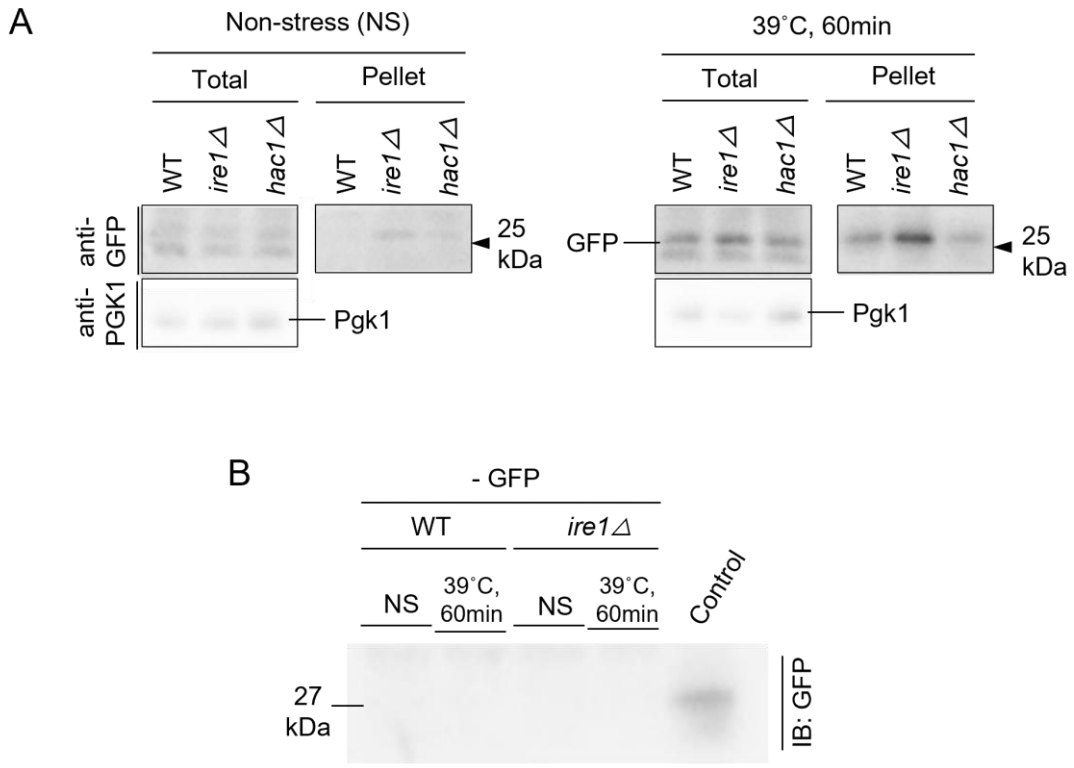

Figure 21: Aggregation of GFP upon heat shock. *P. pastoris* wild-type cells (WT; CBS7435) and its mutants carrying the *ire1⊿0* or *hac1⊿0* mutation were transformed (A) or not transformed (B) with the *GAP1*-promoter driven GFP-expression plasmid, cultured at 30 °C (Non-stress; NS) or shifted to 39°C for 60 min, and harvested. Control sample stated in (B) obtained from *S. cerevisiae* cells expressing GFP. The crude lysates (Total) were then subjected to high-speed centrifugation, and the pellet fractions (Pellet) were obtained. Protein samples (Total: crude lysates corresponding to 6 µg protein; Pellet: preparation from crude lysates corresponding to 16 µg protein) were separated by SDS-PAGE, and the resulting gels were subjected to anti-GFP Western blotting and control Pgk1.

In the experiment shown in Fig. 22, we examined growth of cells on agar plates at different temperatures. All the strains were unable to grow at 39 °C (Fig. 22B). This agar plate was then shifted from 39 °C to 30 °C, resulting in the growth of all strains other than the *ire1Δhac1Δ* strain (Fig. 22C). Therefore, I assume that *IRE1* and *HAC1* confer heat resistance to *P. pastoris* cells in different ways.

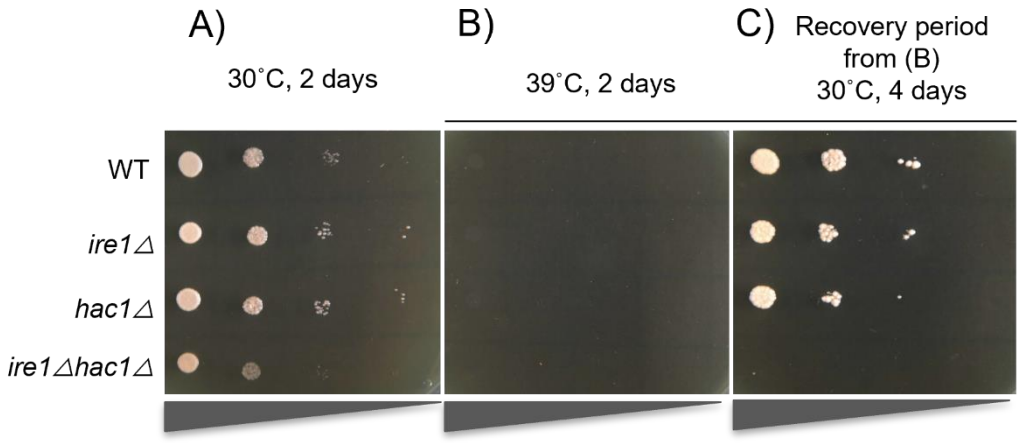

Figure 22: High-temperature sensitivity of *P. pastoris* cells carrying the *ire1Δ* and/or *hac1Δ* mutations. Cultures (OD_{600}=1.0) of *P. pastoris* wild-type cells (WT; CBS7435) and its mutants carrying the *ire1Δ0* and/or *hac1Δ0* mutations were 10-fold serially diluted and spotted onto YPD agar plates. (A) Agar plate was incubated at 30 °C for two days and photographed. (B) Agar plate was incubated at 39 °C for two days and photographed. (C) After incubation at 39 °C for two days, the agar plate was incubated at 30 °C for four days and photographed.

3.9 Relationship between ribosomal proteins and the HSR induction by the *ire1Δ* mutation.

In the final part of my study, I inquired the reason why the *ire1Δ* mutation, but not the *hac1Δ* mutation, aggravates cytosolic and/or nuclear protein aggregation and induces the HSR in *P. pastoris* cells. As aforementioned, ribosomal proteins and factors for ribosomal biogenesis are transcriptionally induced by the *ire1Δ* mutation independently of *HAC1* (Category-B genes). One intriguing hypothesis is that this elevates bulk protein biosynthesis, leading to too much protein load in the cytosol or nuclei, which may induce the HSR. However, this possibility was unsupported by the experiment shown in Fig. 23, where the global protein synthesis did not seem to be different between wild-type and *ire1Δ* cells both under non-stress and heat-shock conditions.

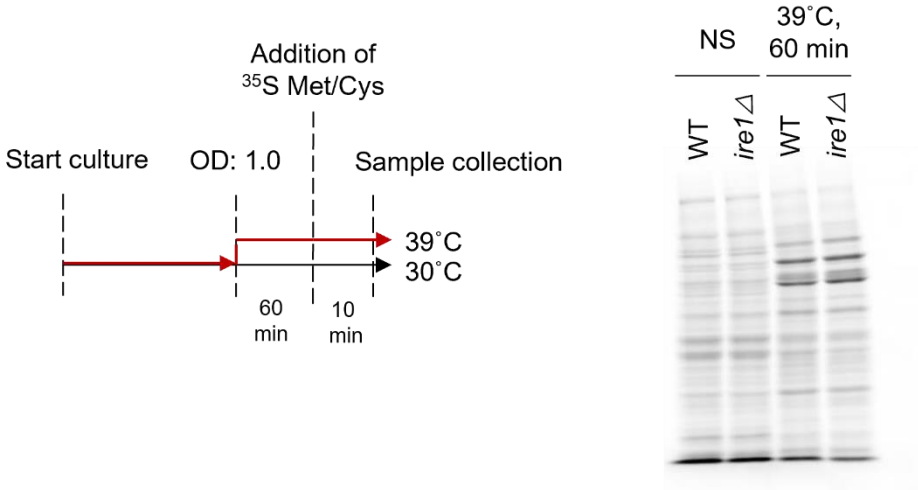

Figure 23: Wild-type and *ire1Δ* mutant cells exhibit similar protein-synthesis properties. After pre-culturing at 30 °C, *P. pastoris* wild-type cells (WT; CBS7435) and its *ire1Δ0* mutant was further cultured at 30 °C (Non-stress; NS) or shifted to 39 °C for 60 min in YPD, radiolabeled with free ^{35}S Met/Cys for 10 min, and harvested. Then total lysates were fractionated by 8% SDS-PAGE, and radiolabeled proteins were visualized by autoradiography.

The MA plot shown in Fig. 24 indicates that many of the ribosomal protein genes were abundantly expressed and induced in *ire1Δhac1Δ* cells compared to *hac1Δ* cells. Therefore, excessively expressed ribosomal proteins can easily trigger the HSR because they may highly accumulated as unassembled proteins in the cytosol and/or nuclei. Indeed, according to a previous report by others [80, 81], aberrant ribosome biogenesis yields unassembled ribosomal proteins, which are proteotoxic and induce the HSR in *S. cerevisiae* cells.

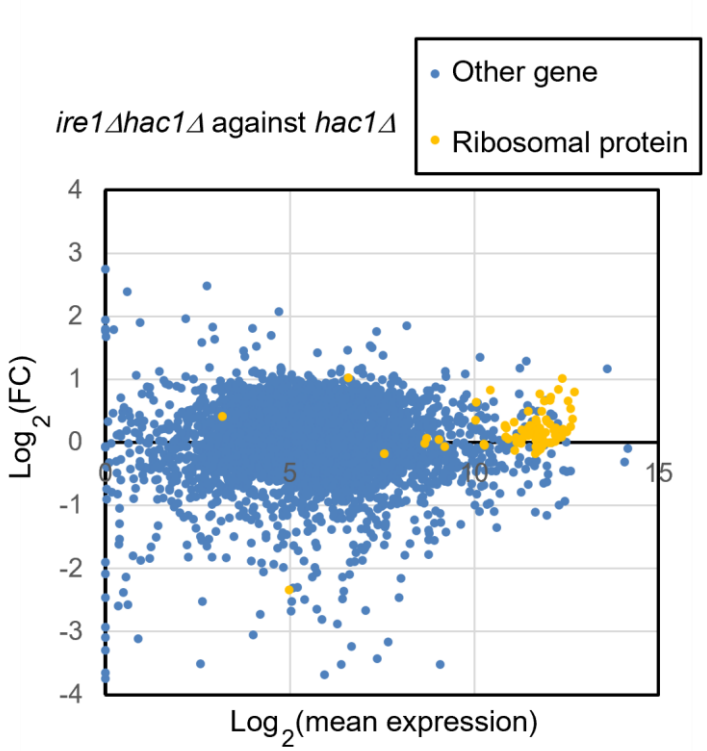

Figure 24: MA plot presentation for DEGs between *ire1Δhac1Δ* and *hac1Δ* cells. The mRNA-seq data shown in Table S1 are expressed as an MA plot, in which the x-axis represents Log_2 of the mean expression level (TPM) and the y-axis represents Log_2 of the FC. FC: Fold change.

CHAPTER 4: DISCUSSION

As described in the Introduction section, *P. pastoris* cells are frequently employed for industrial production of heterologous secretory proteins. Therefore, it is an intriguing question how the ER function is regulated in *P. pastoris* cells, and here I investigated their UPR.

This study revealed that unlike the case of *S. cerevisiae* cells, the UPR is partially but considerably provoked even under non-stress conditions and further induced in response to external ER-stress stimuli in *P. pastoris* cells. This observation is different from those in previous publications by others [62]61]. For instance, according the RT-PCR analysis by Guerfal et al. [62], the *HAC1*u mRNA was virtually undetectable, which means that it was almost perfectly spliced and converted to the *HAC1*i mRNA, even in unstressed *P. pastoris* cells. I deduce that this is due to an experimental bias for which the *HAC1*u mRNA was less efficiently detected than the *HAC1*i mRNA by their RT-PCR analysis [67].

Here I demonstrated that the *P. pastoris*/*S. cerevisiae* chimeric Ire1 mutant was controlled as tightly as the authentic version of *S. cerevisiae* Ire1 when expressed in *S. cerevisiae* cells. I therefore do not infer that the intrinsic regulatory property of *P. pastoris* Ire1 and that of *S. cerevisiae* Ire1 are largely different. Rather, it is likely that *P. pastoris* cells are inherently and naturally ER stressed. According to my colleagues, *P. pastoris* cells secrete far more abundant proteins than *S. cerevisiae* cells, leading to high protein load into the ER [67].

Another notable difference between *P. pastoris* cells and *S. cerevisiae* cells is that as I revealed in this study, *IRE1* and *HAC1* play both interdependent and independent roles in *P. pastoris* cells. On the other hand, as described in the Introduction section, the functions of *IRE1* and *HAC1* are highly interdependent in the case *S. cerevisiae*.

Category A is a group of genes induced by the traditional UPR, for which *IRE1* and *HAC1* cooperatively functions (Fig. 14). Genes in category A include those encoding ER-located molecular chaperone (*LHS1*), factors for disulfide-bond formation in the ER (*ERO1*, *PDI1*), factors for glycosylation (*DPM1*, *OST3*, *ALG2*, *ALG7*), and factors for protein translocation into the ER (*SEC61*, *SEC62*). I deduce that the Category-A genes are those transcriptionally induced by the translation product of the *HAC1*i mRNA, which acts as a nuclear transcription factor. By using DNA microarray technique, Graf et al. [82] listed genes that were induced by DTT treatment

and by artificial expression of the *HAC1*i mRNA in *P. pastoris* cells. As expected, Category-A genes were included in Grafs' list. The number of genes in Category A was smaller than those in Grafs' list, probably because in my case, *P. pastoris* cells are cultured under non-stress conditions, provoking the UPR only moderately.

Moreover, the list of Category-A genes overlaps to that of the UPR target genes in *S. cerevisiae* cells [27, 83]. In this context, the UPR in *P. pastoris* cells and that in *S. cerevisiae* cells have the same biological meaning to enhance activity of the ER and the protein secretory pathway. Nevertheless, it should be also noted that the UPR target genes in these two species are not exactly identical. For instance, membrane-lipid biosynthesis genes, such as *INO1* and *SCS3*, are not induced by the UPR in *P. pastoris* cells (Tables S1 and S2). Unlike the case of *S. cerevisiae* cells [71, 84], expansion of ER membrane may not be an outcome of the UPR in *P. pastoris* cells.

Meanwhile, the main argument of my present study is that in *P. pastoris* cells, Ire1 also functions independently of *HAC1*. Here we note that the *ire1Δ* mutation but not the *hac1Δ* mutation provoked the HSR and protein aggregation. Because at least partly, aggregated proteins are ubiquitylated, I assume that they are formed in the cytosol and/or the nuclei. Therefore, it is likely that in *P. pastoris* cells carrying the *ire1Δ* mutation, cytosolic and/or nuclear protein aggregation leads to evocation of the HSR. To the best of my knowledge, the role of Ire1 to suppress cytosolic and/or nuclear protein aggregation and the HSR, which is illustrated in Fig. 25, has not been previously reported in any eukaryotic species.

Category B is a group of genes that are induced by the *ire1Δ* mutation in the *hac1Δ* background (Fig. 15). Probably because the *ire1Δ* mutation provoked the HSR only modestly, some genes that are deduced to be heat shock genes, namely genes for cytosolic molecular chaperones and their co-factors, did not fall into Category B. Nevertheless, Category B is composed of a number of other genes, which include those encoding ribosomal proteins and ribosome biogenesis factors. According to Tye et al. [81], aberrant ribosome biogenesis yields unassembled ribosomal proteins, which are proteotoxic and induces the HSR to alleviate translational stress [85]. It is therefore possible that Ire1 suppress expression of ribosomal proteins and ribosome biogenesis, leading to attenuation of the HSR.

Some genes related to the proteasome and ubiquitylation were also grouped into Category B. Upregulation of the ubiquitin/proteasome-dependent protein-degradation pathway may be a cellular response to cope with cytosolic and/or nuclear protein aggregation [86].

Nevertheless, it is still unclear what is the proximal role of Ire1 besides splicing the *HAC1* mRNA in *P. pastoris* cells. One possibility is the RIDD, through which Ire1 decreases cellular abundance of specific mRNAs, many of which encode ER-client proteins, independently of *HAC1* [87]. Indeed, as aforementioned, the *ire1Δ* mutation increased expression of a number of genes, namely the Category-B genes, in the *hac1Δ* background. However, it should be also noted that genes for ER-client proteins did not enrich in Category B. Moreover, according to structure prediction by Weihan et al. [88], the RNase domain of *P. pastoris* Ire1, as well as that of *S. cerevisiae* Ire1, has a narrow substrate specificity and is unlikely to perform the RIDD. On the other hand, as proposed in a study on mammalian cells [39], it may be also possible that the kinase domain of Ire1 performs not only auto-phosphorylation but also phosphorylation of other proteins.

As shown in Fig. 18, the *ire1Δ* mutation retarded cellular growth even under the *hac1Δ* background. This observation supports physiological importance of the *HAC1*-independent function of Ire1 in *P. pastoris* cells. Since Ire1 is widely believed to be a factor to cope with ER stress, it sounds an intriguing question what is physiological meaning of the role of Ire1 to mitigate cytosolic and/or nuclear protein aggregation and the HSR. According to Hamdan et al. [89], ER stress totally damages cellular protein-folding status, leading to protein aggregation not only in the ER but also in the cytosol, in *S. cerevisiae*. On the other hand, in some human neurodegenerative diseases including Parkinson's disease, proteins aggregated in the cytosol are thought to trigger ER stress [90]. In other words, cytosolic protein aggregation can be a cause and an outcome of ER stress.

In this study, we also demonstrated another intriguing relationship between the UPR and the HSR. Based on our observation shown in Fig. 19, I propose that high sensitivity of UPR-deficient cells to ER stress can be partly rescued by induction of the HSR in *P. pastoris* cells as well as in *S. cerevisiae* cells [91]. It is uncertain if this observation can be explained solely by expression level of *KAR2*, which is positively regulated both by the UPR and the HSR.

Meanwhile, according to our observations presented here, not only Ire1 but also *HAC1* plays a role(s) other than performing the traditional UPR, in which Ire1 splices the *HAC1* mRNA, in *P. pastoris* cells. Since *HAC1* worked both dependently and independently of Ire1, I assume not only the *HAC1*i mRNA but also the *HAC1*u mRNA has a biological function(s), which should be addressed in future studies.

Since in general, high temperature impairs protein folding, it sounds reasonable that heat stress induces both the HSR and the UPR. Nevertheless, the UPR is only slightly induced at high temperature in *S. cerevisiae* cells [92]. On the other hand, here I exhibited strong activation of Ire1 in heat-stressed *P. pastoris* cells (Fig. 20). Expression pattern of the UPR marker gene *PDI1* was elevated by the temperature shift from 30 °C to 39 °C dependently on both *IRE1* and *HAC1*. Moreover, this temperature shifts strongly induced the HSR, which was mitigated by Ire1. I also demonstrated involvement of Ire1 in heat resistance of *P. pastoris* cells (Fig. 22).

Also in plant cells, heat stress considerably activates Ire1, which then splices the bZIP60 mRNA [31, 93]. Moreover, bZIP60 induces a transcription factor HSFTF13, which upregulates the HSR [94]. Therefore, unlike the case of *P. pastoris*, bZIP60 contributes to induction of the HSR under heat stress conditions in plant cells.

In conclusion, here we disclosed a new role of Ire1 through genetic analyses of *P. pastoris* cells. Besides splicing of the *HAC1* mRNA, Ire1 suppressed cytosolic and/or nuclear protein aggregation and the HSR possibly through avoiding excessive production of ribosomal proteins (Fig. 24). This role of Ire1 to mitigate the HSR was observed also under heat stress conditions, and Ire1 conferred heat resistance to *P. pastoris* cells. Further studies are required to elucidate how widely this insight is applicable to other yeast and fungal species.

As described in the Introduction section, some attempts have been accomplished to improve the ER functions and the heterologous secretory-protein production through genetically modifying the *HAC1* gene in *P. pastoris* cells [60, 95]. On the other hand, here I note that at least in *P. pastoris* cells, *IRE1* has considerably different role from that of *HAC1*. Therefore, genetic manipulations of the *IRE1* gene may confer another outcome, which may also be beneficial for the industrial usage of *P. pastoris* cells.

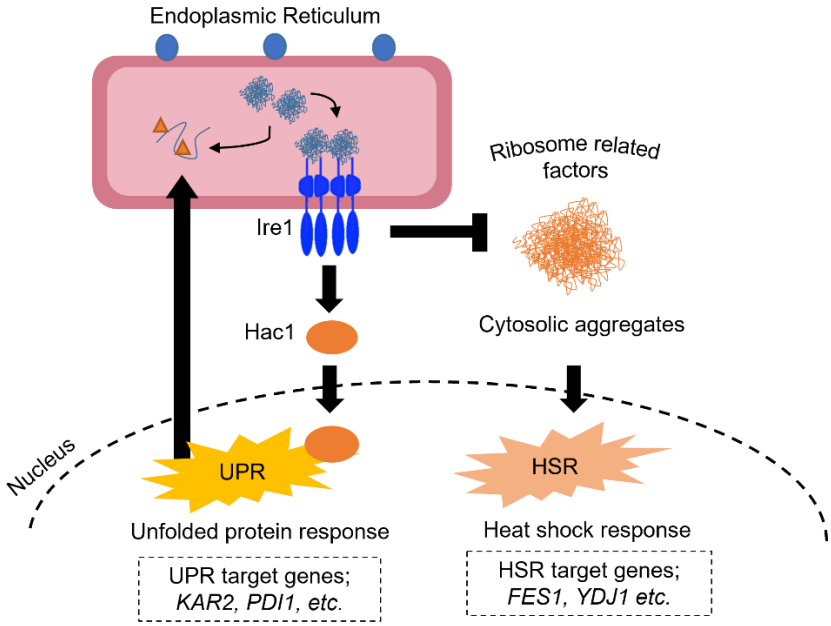

Figure 25: Ire1 has multiple roles in *P. pastoris* cells.

SUPPLEMENTAL MATERIALS

Table S1: Total data of the mRNA-seq analysis
Total TPM data and some relevant values are indicated. Unexpressed genes (TPM = 0.00) were deleted from the list.

Table S2: List of the named genes grouped into Category A, B, or C

The supplemental materials are available at the following site.
https://www.dropbox.com/sh/3hie0gsrbby3a1l/AABha5mDSq9SWlsYhycwiHyOa?dl=0

ACKNOWLEDGEMENT

I would like to thank the following people who have helped me undertake this research:

Associate Professor; Yukio Kimata, my research supervisor, for his constructive and valuable advice throughout the research work. His guidance and endless support had open doors of learning opportunity besides keeping my progress on track.

My advisors; Professor Katsutomo Okamura and Professor Shosuke Yoshida for their time and valuable commentary which help to improve my research.

Dr. Yuki Ishiwata-Kimata for her support and research advice. Her assistance is much appreciated.

All laboratory's members for offering me help and making the stay enjoyable.

The Ministry of Education, Culture, Sports, Science and Technology, Japan for offering the MEXT Scholarship that enabled this research to be possible.

My family and friends for their encouragement and understanding which truly a huge blessing.

Yasmin

REFERENCES

1. Alberts, B., et al., *Essential Cell Biology*. 2013: CRC Press.
2. Cooper, G.M. and R.E. Hausman, *The Cell A Molecular Approach, 4th Ed. + Lecture Notebook*. 2007: Sinauer Associates Incorporated.
3. Yoshida, H., *ER stress and diseases.* The FEBS journal, 2007. **274**(3): p. 630-658.
4. Urra, H., et al., *When ER stress reaches a dead end.* Biochimica et Biophysica Acta (BBA)-Molecular Cell Research, 2013. **1833**(12): p. 3507-3517.
5. Hetz, C., *The unfolded protein response: controlling cell fate decisions under ER stress and beyond.* Nature reviews Molecular cell biology, 2012. **13**(2): p. 89-102.
6. Polizzi, K.M. and C. Kontoravdi, *Genetically-encoded biosensors for monitoring cellular stress in bioprocessing.* Current opinion in biotechnology, 2015. **31**: p. 50-56.
7. Wakabayashi, S. and H. Yoshida, *The essential biology of the endoplasmic reticulum stress response for structural and computational biologists.* Computational and structural biotechnology journal, 2013. **6**(7): p. e201303010.
8. Meusser, B., et al., *ERAD: the long road to destruction.* Nature cell biology, 2005. **7**(8): p. 766-772.
9. Vashist, S. and D.T. Ng, *Misfolded proteins are sorted by a sequential checkpoint mechanism of ER quality control.* The Journal of cell biology, 2004. **165**(1): p. 41-52.
10. Xie, W. and D.T. Ng. *ERAD substrate recognition in budding yeast*. in *Seminars in cell & developmental biology*. 2010. Elsevier.
11. Cox, J.S. and P. Walter, *A novel mechanism for regulating activity of a transcription factor that controls the unfolded protein response.* Cell, 1996. **87**(3): p. 391-404.
12. Määttänen, P., et al. *Protein quality control in the ER: the recognition of misfolded proteins*. in *Seminars in cell & developmental biology*. 2010. Elsevier.
13. Okamura, K., et al., *Dissociation of Kar2p/BiP from an ER sensory molecule, Ire1p, triggers the unfolded protein response in yeast.* Biochemical and biophysical research communications, 2000. **279**(2): p. 445-450.
14. Kimata, Y., et al., *Genetic evidence for a role of BiP/Kar2 that regulates Ire1 in response to accumulation of unfolded proteins.* Molecular biology of the cell, 2003. **14**(6): p. 2559-2569.
15. Kimata, Y., et al., *A role for BiP as an adjustor for the endoplasmic reticulum stress-sensing protein Ire1.* The Journal of cell biology, 2004. **167**(3): p. 445-456.

16. Credle, J.J., et al., *On the mechanism of sensing unfolded protein in the endoplasmic reticulum.* Proceedings of the National Academy of Sciences, 2005. **102**(52): p. 18773-18784.
17. Kimata, Y., et al., *Two regulatory steps of ER-stress sensor Ire1 involving its cluster formation and interaction with unfolded proteins.* The Journal of cell biology, 2007. **179**(1): p. 75-86.
18. Gardner, B.M. and P. Walter, *Unfolded proteins are Ire1-activating ligands that directly induce the unfolded protein response.* Science, 2011. **333**(6051): p. 1891-1894.
19. Mathuranyanon, R., et al., *Tight regulation of the unfolded protein sensor Ire1 by its intramolecularly antagonizing subdomain.* Journal of Cell Science, 2015. **128**(9): p. 1762-1772.
20. Le, Q.G. and Y. Kimata, *Multiple ways for stress sensing and regulation of the endoplasmic reticulum-stress sensors.* Cell Structure and Function, 2021. **46**(1): p. 37-49.
21. Shamu, C.E. and P. Walter, *Oligomerization and phosphorylation of the Ire1p kinase during intracellular signaling from the endoplasmic reticulum to the nucleus.* The EMBO journal, 1996. **15**(12): p. 3028-3039.
22. Sidrauski, C. and P. Walter, *The transmembrane kinase Ire1p is a site-specific endonuclease that initiates mRNA splicing in the unfolded protein response.* Cell, 1997. **90**(6): p. 1031-1039.
23. Korennykh, A.V., et al., *The unfolded protein response signals through high-order assembly of Ire1.* Nature, 2009. **457**(7230): p. 687-693.
24. Mori, K., et al., *A 22 bp cis - acting element is necessary and sufficient for the induction of the yeast KAR2 (BiP) gene by unfolded proteins.* The EMBO journal, 1992. **11**(7): p. 2583-2593.
25. Mori, K., et al., *Signalling from endoplasmic reticulum to nucleus: transcription factor with a basic - leucine zipper motif is required for the unfolded protein - response pathway.* Genes to Cells, 1996. **1**(9): p. 803-817.
26. Kawahara, T., et al., *Endoplasmic reticulum stress-induced mRNA splicing permits synthesis of transcription factor Hac1p/Ern4p that activates the unfolded protein response.* Molecular biology of the cell, 1997. **8**(10): p. 1845-1862.
27. Travers, K.J., et al., *Functional and genomic analyses reveal an essential coordination between the unfolded protein response and ER-associated degradation.* Cell, 2000. **101**(3): p. 249-258.
28. Ogawa, N. and K. Mori, *Autoregulation of the HAC1 gene is required for sustained activation of the yeast unfolded protein response.* Genes to Cells, 2004. **9**(2): p. 95-104.

29. Yoshida, H., et al., *XBP1 mRNA is induced by ATF6 and spliced by IRE1 in response to ER stress to produce a highly active transcription factor.* Cell, 2001. **107**(7): p. 881-891.
30. Calfon, M., et al., *IRE1 couples endoplasmic reticulum load to secretory capacity by processing the XBP-1 mRNA.* Nature, 2002. **415**(6867): p. 92-96.
31. Deng, Y., et al., *Heat induces the splicing by IRE1 of a mRNA encoding a transcription factor involved in the unfolded protein response in Arabidopsis.* Proceedings of the National Academy of Sciences, 2011. **108**(17): p. 7247-7252.
32. Nagashima, Y., et al., *Arabidopsis IRE1 catalyses unconventional splicing of bZIP60 mRNA to produce the active transcription factor.* Scientific reports, 2011. **1**(1): p. 29.
33. Hernández-Elvira, M., et al., *The unfolded protein response pathway in the yeast Kluyveromyces lactis. a comparative view among yeast species.* Cells, 2018. **7**(8): p. 106.
34. Papa, F.R., et al., *Bypassing a kinase activity with an ATP-competitive drug.* Science, 2003. **302**(5650): p. 1533-1537.
35. Chawla, A., et al., *Attenuation of yeast UPR is essential for survival and is mediated by IRE1 kinase.* Journal of Cell Biology, 2011. **193**(1): p. 41-50.
36. Rubio, C., et al., *Homeostatic adaptation to endoplasmic reticulum stress depends on Ire1 kinase activity.* Journal of Cell Biology, 2011. **193**(1): p. 171-184.
37. Le, Q.G., et al., *The ADP-binding kinase region of Ire1 directly contributes to its responsiveness to endoplasmic reticulum stress.* Scientific Reports, 2021. **11**(1): p. 1-14.
38. Lee, K.P., et al., *Structure of the dual enzyme Ire1 reveals the basis for catalysis and regulation in nonconventional RNA splicing.* Cell, 2008. **132**(1): p. 89-100.
39. Urano, F., et al., *Coupling of stress in the ER to activation of JNK protein kinases by transmembrane protein kinase IRE1.* science, 2000. **287**(5453): p. 664-666.
40. Nishitoh, H., et al., *ASK1 is essential for endoplasmic reticulum stress-induced neuronal cell death triggered by expanded polyglutamine repeats.* Genes & development, 2002. **16**(11): p. 1345-1355.
41. Hollien, J. and J.S. Weissman, *Decay of endoplasmic reticulum-localized mRNAs during the unfolded protein response.* Science, 2006. **313**(5783): p. 104-107.
42. Han, D., et al., *IRE1α kinase activation modes control alternate endoribonuclease outputs to determine divergent cell fates.* Cell, 2009. **138**(3): p. 562-575.

43. Morohashi, K.-i. and T. Omura, *Tissue-specific transcription of P-450 (11β) gene in vitro.* The Journal of Biochemistry, 1990. **108**(6): p. 1050-1056.
44. Mishiba, K.-i., et al., *Defects in IRE1 enhance cell death and fail to degrade mRNAs encoding secretory pathway proteins in the Arabidopsis unfolded protein response.* Proceedings of the National Academy of Sciences, 2013. **110**(14): p. 5713-5718.
45. Upton, J.-P., et al., *IRE1α cleaves select microRNAs during ER stress to derepress translation of proapoptotic Caspase-2.* Science, 2012. **338**(6108): p. 818-822.
46. Kimmig, P., et al., *The unfolded protein response in fission yeast modulates stability of select mRNAs to maintain protein homeostasis.* elife, 2012. **1**: p. e00048.
47. Krishnan, K. and D.S. Askew, *Endoplasmic reticulum stress and fungal pathogenesis.* Fungal biology reviews, 2014. **28**(2-3): p. 29-35.
48. Feng, X., et al., *HacA-independent functions of the ER stress sensor IreA synergize with the canonical UPR to influence virulence traits in Aspergillus fumigatus.* PLoS pathogens, 2011. **7**(10): p. e1002330.
49. Ramírez-Zavala, B., et al., *The protein kinase Ire1 has a Hac1-independent essential role in iron uptake and virulence of Candida albicans.* PLoS pathogens, 2022. **18**(2): p. e1010283.
50. Niwa, M., et al., *Genome-scale approaches for discovering novel nonconventional splicing substrates of the Ire1 nuclease.* Genome Biology, 2005. **6**: p. 1-10.
51. Tam, A.B., A.C. Koong, and M. Niwa, *Ire1 has distinct catalytic mechanisms for XBP1/HAC1 splicing and RIDD.* Cell reports, 2014. **9**(3): p. 850-858.
52. Mori, K., et al., *mRNA splicing-mediated C-terminal replacement of transcription factor Hac1p is required for efficient activation of the unfolded protein response.* Proceedings of the National Academy of Sciences, 2000. **97**(9): p. 4660-4665.
53. Schuldiner, M., et al., *Exploration of the function and organization of the yeast early secretory pathway through an epistatic miniarray profile.* Cell, 2005. **123**(3): p. 507-519.
54. Yamada, Y., et al., *The phylogenetic relationships of methanol-assimilating yeasts based on the partial sequences of 18S and 26S ribosomal RNAs: the proposal of Komagataella gen. nov.(Saccharomycetaceae).* Bioscience, biotechnology, and biochemistry, 1995. **59**(3): p. 439-444.
55. Türkanoğlu Özçelik, A., S. Yılmaz, and M. Inan, *Pichia pastoris promoters.* Recombinant Protein Production in Yeast, 2019: p. 97-112.
56. Ata, Ö., et al., *What makes Komagataella phaffii non-conventional?* FEMS Yeast Research, 2021. **21**(8): p. foab059.

57. Cereghino, G.P.L., et al., *Production of recombinant proteins in fermenter cultures of the yeast Pichia pastoris.* Current opinion in biotechnology, 2002. **13**(4): p. 329-332.
58. Bustos, C., et al., *Advances in Cell Engineering of the Komagataella phaffii Platform for Recombinant Protein Production.* Metabolites, 2022. **12**(4): p. 346.
59. Laukens, B., C. De Wachter, and N. Callewaert, *Engineering the Pichia pastoris N-glycosylation pathway using the GlycoSwitch technology.* Glyco-Engineering: Methods and Protocols, 2015: p. 103-122.
60. Küberl, A., et al., *High-quality genome sequence of Pichia pastoris CBS7435.* Journal of biotechnology, 2011. **154**(4): p. 312-320.
61. Valli, M., et al., *Curation of the genome annotation of Pichia pastoris (Komagataella phaffii) CBS7435 from gene level to protein function.* FEMS yeast research, 2016. **16**(6).
62. Guerfal, M., et al., *The HAC1 gene from Pichia pastoris: characterization and effect of its overexpression on the production of secreted, surface displayed and membrane proteins.* Microbial cell factories, 2010. **9**(1): p. 49.
63. Raschmanová, H., et al., *Engineering of the unfolded protein response pathway in Pichia pastoris: enhancing production of secreted recombinant proteins.* Applied Microbiology and Biotechnology, 2021. **105**(11): p. 4397-4414.
64. Whyteside, G., et al., *Activation of the unfolded protein response in Pichia pastoris requires splicing of a HAC1 mRNA intron and retention of the C-terminal tail of Hac1p.* FEBS letters, 2011. **585**(7): p. 1037-1041.
65. Wu, S. and G.J. Letchworth, *High efficiency transformation by electroporation of Pichia pastoris pretreated with lithium acetate and dithiothreitol.* Biotechniques, 2004. **36**(1): p. 152-154.
66. Gassler, T., et al., *CRISPR/Cas9-mediated homology-directed genome editing in Pichia pastoris.* Recombinant protein production in yeast, 2019: p. 211-225.
67. Fauzee, Y.N.B.M., et al., *The unfolded protein response in Pichia pastoris without external stressing stimuli.* FEMS Yeast Research, 2020. **20**(7): p. foaa053.
68. Yang, J., et al., *Hygromycin - resistance vectors for gene expression in Pichia pastoris.* Yeast, 2014. **31**(4): p. 115-125.
69. Promlek, T., et al., *Membrane aberrancy and unfolded proteins activate the endoplasmic reticulum stress sensor Ire1 in different ways.* Molecular biology of the cell, 2011. **22**(18): p. 3520-3532.
70. Tran, D.M., et al., *The unfolded protein response alongside the diauxic shift of yeast cells and its involvement in mitochondria enlargement.* Scientific Reports, 2019. **9**(1): p. 1-14.

71. Nguyen, P.T.M., Y. Ishiwata-Kimata, and Y. Kimata, *Fast-Growing Saccharomyces cerevisiae Cells with a Constitutive Unfolded Protein Response and Their Potential for Lipidic Molecule Production.* Applied and Environmental Microbiology, 2022. **88**(21): p. e01083-22.
72. Li, Z., et al., *Low-temperature increases the yield of biologically active herring antifreeze protein in Pichia pastoris.* Protein Expression and Purification, 2001. **21**(3): p. 438-445.
73. Gasser, B., et al., *Monitoring of transcriptional regulation in Pichia pastoris under protein production conditions.* BMC genomics, 2007. **8**(1): p. 1-18.
74. Kimata, Y. and K. Kohno, *Endoplasmic reticulum stress-sensing mechanisms in yeast and mammalian cells.* Current opinion in cell biology, 2011. **23**(2): p. 135-142.
75. Kohno, K., et al., *The promoter region of the yeast KAR2 (BiP) gene contains a regulatory domain that responds to the presence of unfolded proteins in the endoplasmic reticulum.* Molecular and cellular biology, 1993. **13**(2): p. 877-890.
76. Morano, K.A., P.C. Liu, and D.J. Thiele, *Protein chaperones and the heat shock response in Saccharomyces cerevisiae.* Current opinion in microbiology, 1998. **1**(2): p. 197-203.
77. Chen, S. and G. Qiu, *Heat-stress induced expression of stress-inducible nucleotide exchange factor Fes1 in seagrass Zostera japonica.* Ecotoxicology, 2020. **29**(7): p. 932-940.
78. Klaips, C.L., et al., *Sis1 potentiates the stress response to protein aggregation and elevated temperature.* Nature communications, 2020. **11**(1): p. 6271.
79. Masser, A.E., et al., *Cytoplasmic protein misfolding titrates Hsp70 to activate nuclear Hsf1.* Elife, 2019. **8**: p. e47791.
80. Sung, M.-K., et al., *A conserved quality-control pathway that mediates degradation of unassembled ribosomal proteins.* Elife, 2016. **5**: p. e19105.
81. Tye, B.W., et al., *Proteotoxicity from aberrant ribosome biogenesis compromises cell fitness.* elife, 2019. **8**: p. e43002.
82. Graf, A., et al., *Novel insights into the unfolded protein response using Pichia pastoris specific DNA microarrays.* BMC genomics, 2008. **9**(1): p. 1-13.
83. Kimata, Y., et al., *Yeast unfolded protein response pathway regulates expression of genes for anti‐oxidative stress and for cell surface proteins.* Genes to Cells, 2006. **11**(1): p. 59-69.
84. Schuck, S., et al., *Membrane expansion alleviates endoplasmic reticulum stress independently of the unfolded protein response.* Journal of Cell Biology, 2009. **187**(4): p. 525-536.

85. Brandman, O., et al., *A ribosome-bound quality control complex triggers degradation of nascent peptides and signals translation stress.* Cell, 2012. **151**(5): p. 1042-1054.
86. Sung, M.-K., et al., *Ribosomal proteins produced in excess are degraded by the ubiquitin–proteasome system.* Molecular biology of the cell, 2016. **27**(17): p. 2642-2652.
87. Coelho, D.S. and P.M. Domingos, *Physiological roles of regulated Ire1 dependent decay.* Frontiers in genetics, 2014. **5**: p. 76.
88. Li, W., et al., *Protomer alignment modulates specificity of RNA substrate recognition by Ire1.* Elife, 2021. **10**: p. e67425.
89. Ali, M., et al., *Stress-dependent proteolytic processing of the actin assembly protein Lsb1 modulates a yeast prion.* Journal of Biological Chemistry, 2014. **289**(40): p. 27625-27639.
90. Melo, T.Q., S.J. Copray, and M.F. Ferrari, *Alpha-synuclein toxicity on protein quality control, mitochondria and endoplasmic reticulum.* Neurochemical research, 2018. **43**: p. 2212-2223.
91. Liu, Y. and A. Chang, *Heat shock response relieves ER stress.* The EMBO journal, 2008. **27**(7): p. 1049-1059.
92. Hata, T., Y. Ishiwata-Kimata, and Y. Kimata, *Induction of the unfolded protein response at high temperature in Saccharomyces cerevisiae.* International Journal of Molecular Sciences, 2022. **23**(3): p. 1669.
93. Li, Y., S. Humbert, and S.H. Howell, *ZmbZIP60 mRNA is spliced in maize in response to ER stress.* BMC Research Notes, 2012. **5**: p. 1-11.
94. Li, Z., et al., *The transcription factor bZIP60 links the unfolded protein response to the heat stress response in maize.* Plant Cell, 2020. **32**(11): p. 3559-3575.
95. Zahrl, R.J., et al., *Synthetic activation of yeast stress response improves secretion of recombinant proteins.* New Biotechnology, 2023.